JRC Scientific and Technical Reports

Some considerations on continental scale pollutant transport modelling in European marine waters

Alberto Pistocchi, Adolf Stips

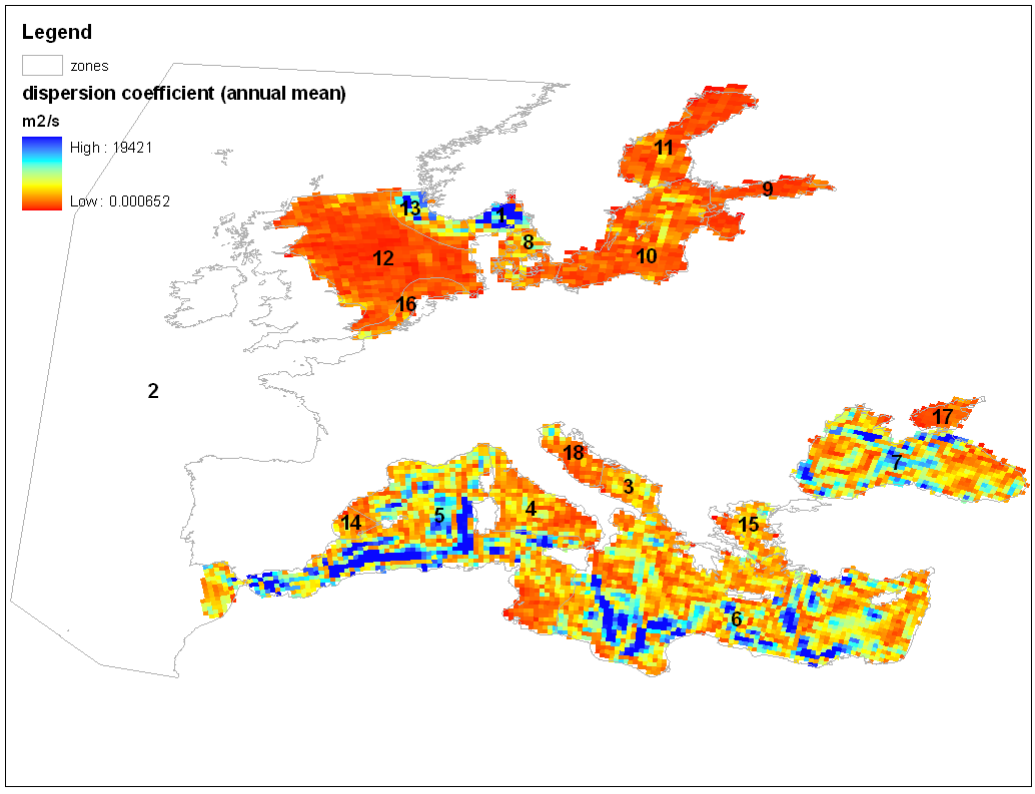

EUROPEAN COMMISSION
JRC
Institute for Environment and Sustainability
EUR 24267 EN - 2010

The mission of the JRC-IES is to provide scientific-technical support to the European Union's policies for the protection and sustainable development of the European and global environment.

European Commission
Joint Research Centre
Institute for Environment and Sustainability

Contact information
Address: Alberto Pistocchi, JRC, TP 460, Via Fermi 2749, 21027 Ispra (VA), Italy
E-mail: alberto.pistocchi@jrc.ec.europa.eu
Tel.: 00 39 0332 785591
Fax: 00 39 0332 785601

http://ies.jrc.ec.europa.eu/
http://www.jrc.ec.europa.eu/

JRC 56757

EUR 24267 EN
ISBN 978-9279-15067-8
ISSN 1018-5593
DOI 10.2788/66854

Luxembourg: Publications Office of the European Union

Printed in Italy

1. Introduction

A large part of Europe's chemical emissions reaches the oceans and seas through both atmospheric transport and deposition, and direct and indirect water discharges.
The former process is relatively uniform across the continent, especially for chemicals of widespread use and pollution from diffuse sources, when horizontal gradients of contamination are not very steep (e.g. from atmospheric deposition).; in such cases, one-dimensional vertical ("water column") models [e.g.9, 17] allow estimating the partitioning of chemicals between environmental phases, and overall "vertical" fluxes across interfaces (air-water, water-sediments), providing insights on the relative importance of the different processes determining chemical fate.
On the contrary, for emission sources of limited spatial extension such as discharges from rivers or from industrial plants, the transport patterns assume the shape of plumes, and originate relatively steep horizontal gradients of contamination, so that lateral transport cannot be neglected. Within plumes of contamination, concentrations may range across one or more orders of magnitude, which may be of a certain importance when evaluating chemical risks to human health and ecosystems.
In such cases, a comprehensive two- or three-dimensional seawater circulation and contaminant transport model remains the elective tool for the simulation of pollution. In the last decades, comprehensive hydrodynamic numerical models have been developed for many areas in the world. Using numerical models allows exploring ocean processes beyond crude experimental observations through a consistent, continuous representation of processes [51], which enables identifying dominant and persistent flow patterns, advective and dispersive parameters controlling the transport of contaminants. Among many other studies, a hydrodynamic model has been implemented for the European seas [13, 52, 37], using the GETM code [5], which provides a homogeneous description of seawater dynamics for the whole continent.
However, models of this kind are computationally demanding and require considerable data input in order to be properly calibrated and validated. Therefore, direct use of such model may be impractical for quick fate and transport calculations under high uncertainties about emissions and environmental behaviour of chemicals.
For practical purposes, it may be of interest to develop screening level tools, which may be applied with minimal data input or standard data sets, in order to perform preliminary assessment over large numbers of chemicals, when uncertainties in their emissions and environmental behaviour are relatively high, and when aiming at a quantification of impacts over large regions rather than a detailed, site specific simulation of physical processes.
One strategy to simplify models is dimensional reduction of the problem. For instance, concentrations in seawater predicted by the EMEP MSCE-POP model [3] for polychlorobiphenyls, dioxins and furans are well correlated to atmospheric deposition, although the model includes lateral transport (see Figure 1), suggesting that a one-dimensional model would yield equally good results [e.g. 39]. In a study on the English Channel [30], a question was posed about the real advantages of using complex three dimensional models compared to simpler box models. Along this line, spatially explicit models have been developed describing the geographical distribution of chemicals (e.g. [38, 21, 43, 25, 35]), which also take into account the seawater compartment. These models subdivide the seawater compartment into a number of boxes, for each computing mass balance depending on "vertical" processes (typically, volatilization, particle settling, and degradation) and "lateral" ones (advection and dispersion).
Developing simple models is often not a choice, but a necessity when describing the fate and transport of chemicals in seawaters. This is the case when information about emissions, physico-chemical properties, and environmental parameters do not allow nor justify time-consuming, accurate simulations and one is rather interested in order-of-magnitude calculations and the identification of the relative importance of different processes. This is true in particular for many persistent organic pollutants (POPs), as well as for many industrial or agri-chemicals posing concerns for marine ecosystems. For certain purposes, such as overall mass balance of substances, very simple box models,

such as the one presented by Gomez [12] for the Mediterranean, have been used. Widely adopted assessment guidelines, among which the European Commission Technical Guidance Document (TGD) on risk assessment and the LOICZ mass balance methodology suggest to compute expected concentrations in the coastal zone of a chemical derived from inland sources, using a continuous stirred tank reactor or box model; the LOICZ methodology suggests using an ad hoc definition of the box volume and residence time; the TGD proposes a seawater compartment volume defined by a coastal current velocity and a dispersion coefficient (or equivalently alongshore and cross-shore mixing distances). Although examples are provided of suitable values for current velocity and dispersion coefficient, little general guidance is provided about the selection of such parameters under varied geographic conditions. Moreover, while box models enable computing a concentration in the coastal zone, they do not account for the transport of contaminants towards the outer sea region, and cannot be used to explicitly map coastal contamination, which is of interest when aiming at a picture of cumulative effects of coastal pollution.

In this paper, we discuss possibilities and limitations in using simple models, as a supplement to existing methods, for screening level predictions at the continental scale when developing complex models would require excessive efforts, yet a spatially explicit mapping of coastal pollution is required.

The hydrodynamic models for European seas developed at the JRC using the GETM code [13, 52, 37] provide a spatial representation of advection and dispersion processes that, together with improved spatially explicit description of processes such as the air-water exchange [9, 15, 16], and features of the particulate material in seawater [28, 29], provides relevant material for map-based modeling [39].

In this report we make use of the hydrodynamic information from these models to build simple model schemes of seawater transport, in order to discuss the relative importance of vertical and lateral processes (hence the applicability of a “water column” approach for the fate and transport of pollutants), and to model the attenuation of seawater pollution from coastal sources through map calculations.

2. Materials and methods

In this section, we introduce the data we used to develop two simple analytical tools, namely a box model and a model of exponential decay of chemicals with distance from the coast. Subsequently we provide details of the two tools. In the next section we use these tools to develop some quantitative considerations on the appropriateness and limitations of certain choices in the setup of chemical fate models for coastal and marine waters.

2.1 Hydrodynamics of European seas and definition of homogeneous sea zones

As a first step in the analysis, we reconstructed the hydrodynamics of European seas through the aggregation at monthly steps of detailed hydrodynamic model results obtained for the Black Sea [37], Mediterranean [13], North and Baltic Sea [52].

GETM (General Estuarine Transport Model, www.getm.eu) is a recent 3D numerical model which is simulating the most important hydrodynamic and thermodynamic processes in natural waters. The three-dimensional hydrostatic equations of motion are solved by applying the Boussinesq approximation and the eddy viscosity assumption. The model is general in the sense that it can be applied to various systems, scales and specifications. The model includes for example flexible vertical and horizontal coordinate systems, different turbulence models that are integrated from the GOTM (General Ocean Turbulence Model, www.gotm.net), and is a Public Domain model available under the GNU General Public License. Results obtained with the GETM model are published for instance in [52, 51, 2].

Available models for European seas have different resolutions. For the sake of uniformity, model results were homogenized to the resolution of 0.25 degrees, obtaining a set of monthly average values of northerly and easterly flow velocity, and seawater temperature.

The uppermost layer of the ocean is normally referred to as mixed layer, because of the uniform distribution of temperature, salinity and therefore also density. Typically the mixed layer depth (MLD) will be defined as the depth at which the density (temperature) changes by a certain amount from the surface density (temperature).

There is no unique method applied to determine this so called mixed layer depth in oceanographic studies, because of the great regional variability of the density gradient. This tolerance level is individually and regionally adjusted [60]. In order to avoid the necessity of doing such a subjective adjustment for every European Sea, we decided to determine the mixed layer depth from the depth of the maximum density gradient. This method has proved to be very robust without any tuning applied for most of the regional Seas in Europe, except for minor uncertainties in some parts of the Baltic Sea during spring and autumn stratification changes.

The spatial distribution of velocity vectors can be plotted and allows identifying sea zones where water circulation creates gyres (currents for the months of January and July are provided as examples in Figure 2). By visual inspection of the velocity vector plots, a limited number of sea zones can be extracted based on the presence of gyres; as these are generally efficient mixing mechanisms [45], this segmentation allows minimizing the lateral exchanges between zones. At the same time, the presence of gyres inside the zones supports the assumption that full mixing of solutes occurs inside the zone, after a finite time, provided the sources of solutes are sufficiently persistent. There are some cases when it is not possible to identify gyres. This may happen when water velocities are extremely low, or if water flows along a single dominant direction.

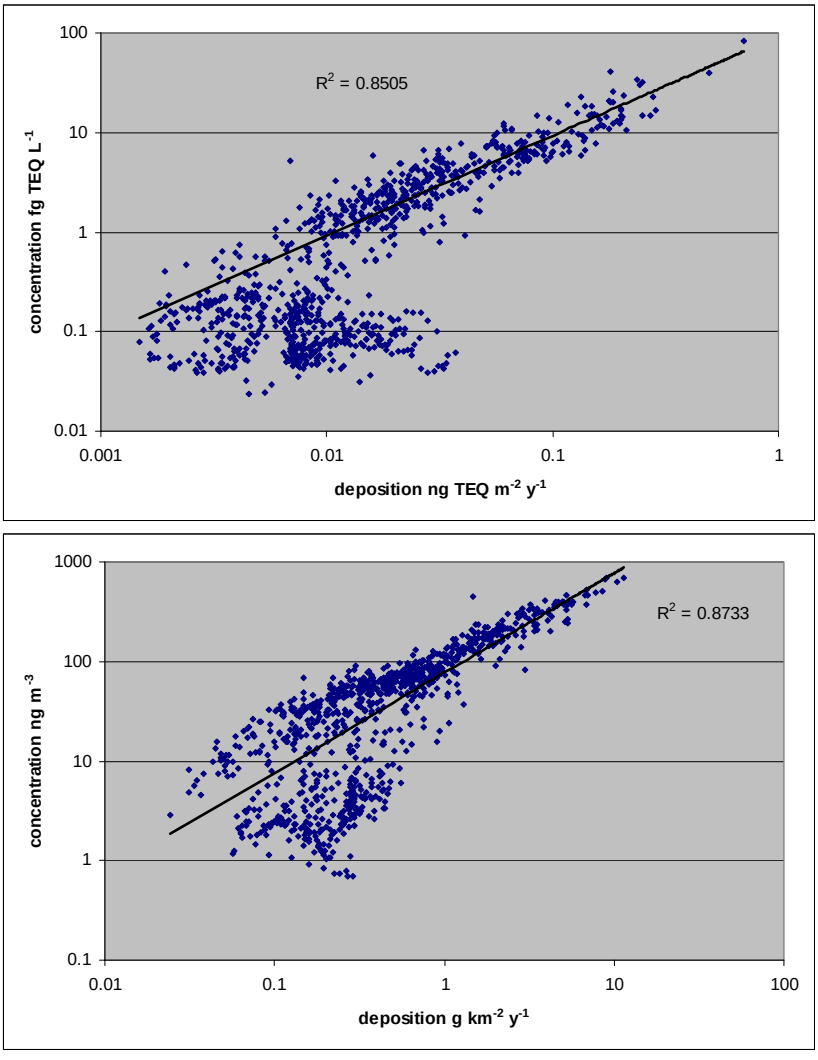

Figure 1 - Scatter diagram and correlation between atmospheric deposition and sea water concentration for PCBs (below) and PCDD/Fs (above) as modelled by the EMEP MSCE-POP model.

In the first case, a zone may be identified as a still water body, where mixing may occur due to dispersion only; in the second case, a zone represents a channel where advection contributes to the transfer of solute and water mass along a specified direction.

Based on the qualitative interpretation of the hydrodynamic model results, we extracted 18 zones (Figure 2). It is worth stressing that, although seasonal variation appears, the currents identified by the hydrodynamic model are rather persistent and can be considered constant year-round as a first approximation. The portion of the Atlantic Ocean relevant for Europe is represented as a single zone (zone #2) which connects the others; for this zone, advection and dispersion parameters are assigned conventionally based on data from [32, 26].

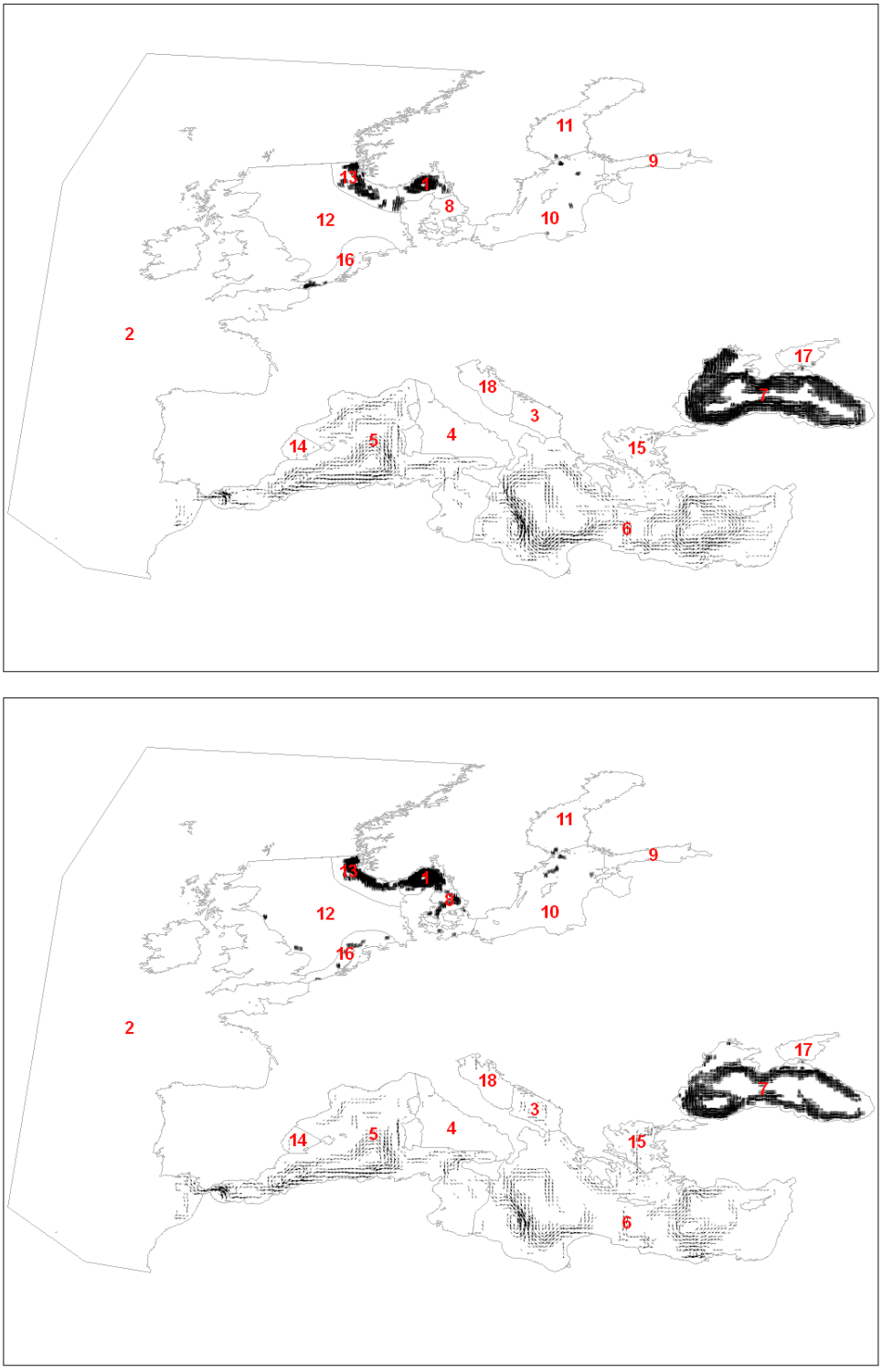

Figure 2 – Hydrodynamics of European seas with the identification of seazones. Above: currents in January; below: currents in July. Velocity vectors with intensity less than 10 cm/s are not represented.

2.2 Multi-box fate and transport model

From the results of the GETM model it is possible to derive information necessary to describe the interaction among zones as a system of continuous stirred tank reactors (CSTRs) or boxes. The mass distribution of a chemical substance can be therefore estimated, under steady state assumptions, by solving a system of linear mass balance equations for the chemical, which can be written in matrix form (e.g. [38,]) as:

$$S - \mathbf{K} M = 0 \qquad (1)$$

where **K** is the rate matrix, M is the mass vector representing the total mass of chemical in each zone, S the source vector representing the net external input of chemical to each zone. This is a level III multi-box model according to Mackay [22, 23]. The rate matrix has diagonal terms as:

$$K_{ii} = K_{i,removal} + K_{i,\ transport} \qquad (2)$$

Where $K_{i,\ removal}$ is the removal rate, including degradation, volatilization and settling of sediment-attached substance, while $K_{i,\ transport} = \sum_{\substack{j=1 \\ j \neq i}}^{n} \frac{P_{ij} Q_{ij}}{V_i} + \sum_{\substack{j=1 \\ j \neq i}}^{n} \frac{P_{ij} J_{ij}}{V_i}$, whereas off-diagonal terms are:

$$K_{ij} = -\frac{P_{ij} Q_{ji}}{V_i} + \frac{P_{ij} J_{ji}}{V_i} \qquad (3)$$

In the above equations, Q_{ij} is the advection mass discharge per unit perimeter of the zone, J_{ij} is the dispersion mass discharge per unit perimeter of the zone, V_i is the volume of zone i and P_{ij} is the length of the portion of the perimeter of zone i adjoining zone j.

Advection mass discharge is estimated by the product of dissolved concentration times water discharge. In this report, we refer for discussion to the annual mean (average of the monthly means) of velocity (Figure 4) and mixed layer depth. Estimates from the literature have been used for exchanges between the North Sea and Atlantic through the English Channel [48], Black Sea and Mediterranean [44], and Mediterranean and Atlantic Ocean [12]. Also, when the GETM model resolution did not allow accurate estimates, literature data were used, as in the case of exchanges across the strait of Messina [1] and the exchange between the Black and the Azov sea [19]. Dispersion mass discharge is estimated using a linear approximation of Fick's law: $J = \frac{hD(C - C_0)}{\Delta X}$, where D is the dispersion coefficient, h is the zone depth, and ΔX is the cell size of the calculation (here, equal to approximately 25 km or 0.25^o).

The dispersion coefficient can be estimated using empirical approaches [36, 7]; however, there is little guidance on the choice of one single empirical model among many, although the implications may be dramatic not so much on the pattern of spatial evolution of the dispersion coefficient, as on the orders of magnitude (see example of Figure 3). Such an indetermination of the orders of magnitude does not allow to use empirical models for the purposes of this study.

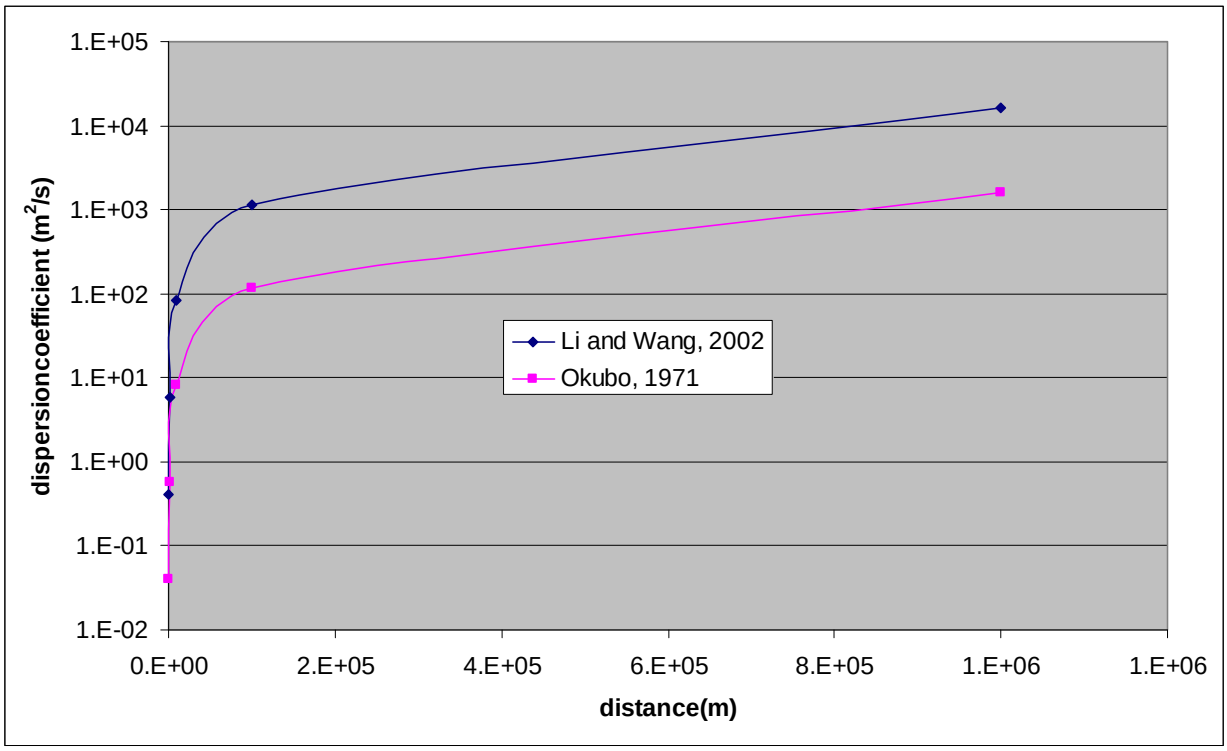

Figure 3 – Comparison of dispersion estimates according to two different empirical models

The dispersion coefficient can be seen as a result of local turbulence in a constant average velocity field; in such case, it is usually described as a function of the scale of the plume size, L, and through statistical mechanics arguments it can be proven to be proportional to $L^{4/3}$ [see e.g.[7], p. 93], although experiments suggest its growth is slower with L and corresponds to an exponent equal to 1.15 [36].
At larger scales, however, average velocity fields are never constant. In such cases, D accounts for transport mechanisms related to the deformation velocity. In particular, the Smagorinsky model [50] can be formulated in a two-dimensional case as:

$$D \propto \left(\frac{\partial U}{\partial y} + \frac{\partial V}{\partial x} \right) (\Delta X)^2$$

where U, V are velocity components in the mixing zone, along x and y directions respectively, and ΔX is the model resolution. Usually, a proportionality constant of 0.04 is assumed. In this case, dispersion does not depend any more on the scale of the plume length, and in zones of small variation of the velocity gradients it maintains a constant value. In this study we referred to the Smagorinsky algorithm in the form:

$$D = 0.04 \sqrt{\left(\frac{\partial U}{\partial y} + \frac{\partial V}{\partial x} \right) \left(\frac{\partial U}{\partial y} + \frac{\partial V}{\partial x} \right)} (\Delta X)^2 \qquad (4)$$

where U, V are velocity components in the mixing zone, along x and y directions respectively, and ΔX is the model grid cell size (in the current implementation, equal to 25 km). Dispersion from annual mean velocity is plotted in Figure 4. In some chemical fate and transport models (e.g. [56]) advective transport is considered negligible in comparison with dispersion at global scale. To evaluate the local relative importance of the two phenomena, we computed a map of the Péclet number:

$$Pe = \frac{\Delta X \sqrt{U^2 + V^2}}{D}. \qquad (5)$$

Figure 5 shows the map histogram, indicating that in most of the European seas advection and dispersion are comparable (Pe in the range 10^{-1}– 10^{1}). We computed a map correlation matrix for the hydrodynamic variables, highlighting that the Péclet number results are spatially poorly correlated with dispersion and velocity, whereas these have a relatively high correlation, as visually highlighted in maps of Figure 4.

	Pe	Dispersion coefficient	Velocity	Depth
Pe	1	-0.03	0.03	-0.01
Dispersion coefficient	-0.03	1	0.45	0.13
Velocity	0.03	0.45	1	0.14
Depth	-0.01	0.13	0.14	1

Table 1 – Correlation matrix of the hydrodynamic variables

The total mass of the chemical M in the bulk of each zone is distributed among water and suspended sediments under the assumption of equilibrium partitioning (e.g. [47]):

$$M = (1 + K_{OW} f_{OC} \iint_A TSM \; h \, dx \, dy) \; C \qquad (6)$$

where TSM is total suspended solids concentration (which should include also biomass), C is dissolved concentration of the chemical, h the mixed zone water depth, K_{ow} is the octanol-water partition coefficient and f_{OC} the fraction of organic carbon in the suspended solids, and A is the area of the zone. Usually, K_{ow} is chemical-specific and homogeneous over the compartment, although its dependence on temperature is sometimes appreciable [3]. Total suspended matter (TSM) has been estimated from SeaWIFS products [28, 29] as described in [42]. In this report, f_{OC} is assigned a constant value of 0.5 [20].

We consider three mechanisms of chemical removal besides transport: degradation (through a constant value of the degradation rate), volatilisation and settling with particles to the deep sea zone.

Volatilisation of the dissolved mass of chemical is described according to the classical double resistance model presented in [47] and widely used in other fate and transport models (e.g. [38, 39]):

$$v_{w-a,diff} = \frac{FR\_DISS}{\left(\frac{1}{v_a'} + \frac{1}{v_w}\right)} \qquad (7)$$

where v'a is the chemical diffusion velocity through air boundary layer [m/s], vw is the chemical diffusion velocity through water boundary layer [m/s], and FR_DISS = $(1 + K_{OW} f_{OC} \iint_A TSM \; h \, dx \, dy)^{-1}$.

We adopt the following relations [47] for the diffusion velocity in air:

$$v_a' = \left(\frac{18}{MW}\right)^{0.335} \cdot K_{aw} \cdot \left(0.002 \cdot u_{10} + 0.003\right) \qquad (8)$$

and in water:

$$v_w = \left(\frac{32}{MW}\right)^{0.285} \cdot \left(0.00004 \cdot u_{10}^2 + 0.0004\right) \qquad (9)$$

where MW is the molecular weight of the chemical and u10 the mean wind speed at 10 m over surface [m/s]; wind speed on the sea surface was taken from [49].

The sink of chemicals with sediment settling to the deep seawater is described through a simple product of the settling velocity of particles, times the sediment phase concentration of the chemical. The settling velocity of particles is assumed to be constantly equal to 1E-4 m/s, which is in the range of values reported in the literature (e.g. [27, 34, 18]). A sensitivity analysis of the model with respect to both f_{OC} and the settling velocity has been done with reference to 5 hazardous priority substances of the Water Framework Directive 60/2000/EC [58] as reported in Table 3 (with the respective physico-chemical properties), highlighting that the removal rates are almost independent on these two parameters for the selected chemicals. It is worth noting that many other parameterization schemes have been proposed elsewhere (e.g. [59]). The average values of the parameters required for the computation of the partitioning and removal rates are shown in Table 2.

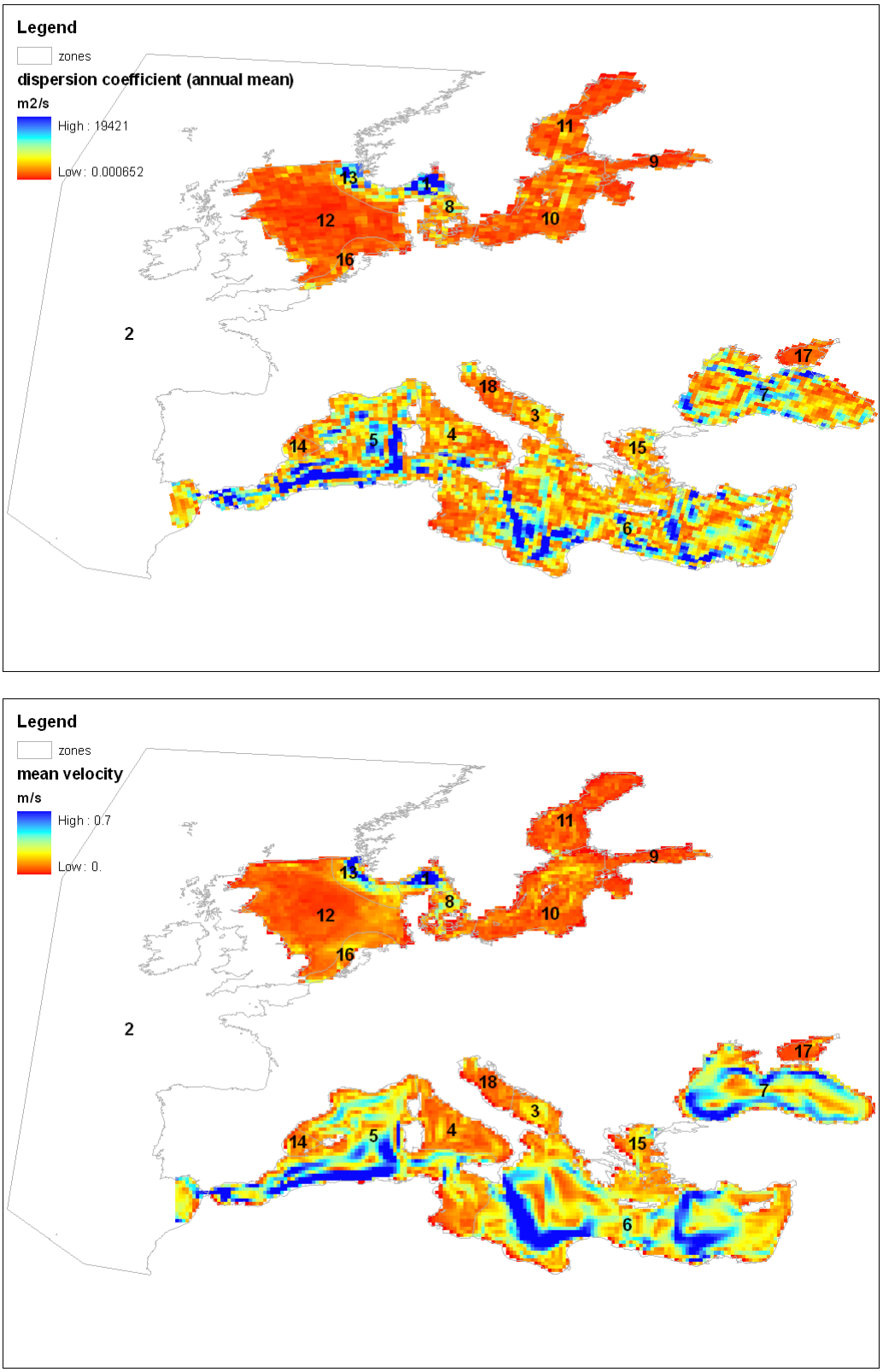

Figure 4 – Spatial distribution of the dispersion coefficient and velocity (annual means)

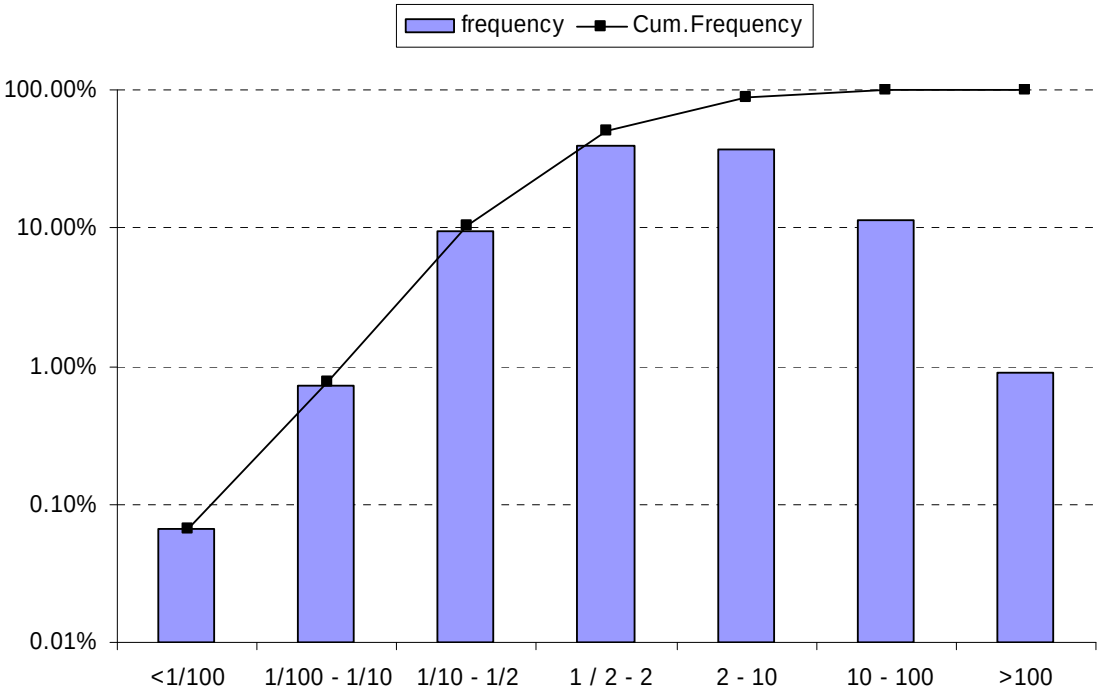

Figure 5 – Frequency distribution of the Peclet number (annual mean)

zone #	perimeter km	area km2	V x d m2/s	(D/ Δs) x d m2/s	d m	u10 m/s	T °C	TSM mg/L (x 100)	*diffusion velocity in air m/s*	*diffusion velocity in seawater m/s*
1	220	38,090	5.82	6.03	30	6.91	10.51	70.0	6.55E-03	1.22E-05
2	470	3,860,000			50	8		54.0	7.40E-03	1.56E-05
3	260	66,920	2.4	2.41	46	4.74	18.27	38.5	4.86E-03	6.86E-06
4	710	180,600	1.6	2.23	45	5.7	18.53	23.7	5.61E-03	8.98E-06
5	1690	789,900	4.9	4.82	43	6.13	18.33	36.9	5.95E-03	1.01E-05
6	890	1,327,000	5.31	4.29	47	5.76	20.01	32.9	5.66E-03	9.13E-06
7	-	427,700	2.75	1.96	21	5.69	14.19	73.5	5.60E-03	8.96E-06
8	200	52,730	0.71	0.47	13	6.86	10.21	109.6	6.52E-03	1.21E-05
9	200	54,570	0.38	0.35	23	6.94	8.1	348.3	6.58E-03	1.23E-05
10	450	219,700	1.18	1.09	37	6.79	9.68	188.3	6.46E-03	1.19E-05
11	130	110,200	0.82	0.8	34	5.93	7.32	196.0	5.79E-03	9.55E-06
12	1200	368,400	0.9	0.72	39.8	7.7	10.8	187.2	7.17E-03	1.46E-05
13	690	64,320	4.92	4.51	44	7.93	10.57	67.2	7.35E-03	1.54E-05
14	500	32,000	1.7	1.87	41	5.2	18.28	26.0	5.22E-03	7.83E-06
15	330	110,100	2.28	2.31	45	6.01	16.96	45.3	5.85E-03	9.75E-06
16	650	62,810	0.8	0.54	18	7.45	12.04	295.7	6.97E-03	1.38E-05
17	-	38,940	0.08	0.09	4	6.27	10.24	391.6	6.06E-03	1.04E-05
18	180	72,610	0.71	0.84	26.38	4.8	16.36	54.6	4.91E-03	6.98E-06

Table 2 – Properties of the 18 European sea zones

The system (1) implemented for the above defined sea zones allows computing mass distribution from a generic distribution of emissions. In particular, the model can be used to estimate source-receptor matrixes, i.e. mass distributions deriving from unit emission in each of the zones. Source-receptor matrixes for the chemicals of Table 3 are available in Excel ® format from the Authors.

The model is based on the assumption that each zone reaches complete mixing. Assuming each zone of area A is approximated as a circle, the length of the circumference of radius equal to half the radius of the zone, $L = \sqrt{\pi A}$, provides a first estimate of the mixing pathway length. The time spent by chemicals along this length due to advective movement can be estimated as $T_{adv} = L/v$, although dispersion of the advective front may affect this estimate [58]. The time required for a cell of given concentration to have it reduced by 90% in the assumption of zero concentration at the far border is $T_{disp} = \frac{\ln 10}{D\Delta X^2}$, ΔX being the cell size. Similarly, the removal time is $T_{rem} = \frac{\ln 10}{k}$ where the overall removal rate k sums degradation, volatilisation and settling rates. In this way, the ratio between mixing times and removal times can be assessed for each sea zone for generic chemicals and particularly the ones of Table 3. Results, shown in Figure 6, indicate that often the time scale of mixing within a zone, and removal are comparable, suggesting that the assumption of a fully mixed zone should be looked at critically, and a variability in concentrations within each zone is to be expected especially for more volatile chemicals. However, most of the times mixing is faster than removal and therefore the model assumption can be accepted as a first approximation.

chemical #	*Name*	*Cas*	*MW*	*Kow*	*Kaw*	*Kdeg hr-1*	*Source*
1	Anthracene	120-12-7	178.2	34673.69	0.001787	0.00126	Impact 2002
2	Hexachlorobenzene	118-74-1	284.79	316227.8	0.032661	1.26E-05	Impact 2002
3	Hexachlorobutadiene	87-68-3	260.76	50118.72	1.005795	0.000407	Impact 2002
4	Endosulfan	115-29-7	406.92	3981.072	0.000427	0.008873	Mackay, 1997
5	Pentachlorobenzene	608-93-5	250.3	100000	0.03421	0.000112	Impact 2002

Table 3 – Chemicals used for the assessment of transport. Data sources correspond to the references Mackay, 1997 [24] and Impact 2002 [38]

2.3 Plume model of pollution from coastal sources

A relevant issue concerning European seas is the importance of pollution from inland sources. Emissions to the sea from sources of limited spatial extension originate a plume of contaminant controlled by removal, advection and dispersion. This plume may take different shape in relation to the local dispersion and advection patterns, and particularly to the direction of the main currents. Under the assumption that dispersion is the only relevant transport mechanism in oceans, a steady state solution of the advection-dispersion-reaction equation, with boundary conditions of given concentration at the coastal boundary and zero mass to infinity takes the form:

$$\frac{C(r)}{C(0)} = f\left(\sqrt{\frac{kr^2}{D}}\right) \qquad (10)$$

where f is a function depending on the geometry of the problem, and r is the distance from the coast. The function f is a modified Bessel function of the second kind for radial propagation, and a simple negative exponential for the case of parallel (one-dimensional) propagation (see e.g. [55], pp 486-487). In real cases of propagation of contaminants, e.g. from a river mouth, it is likely that an intermediate situation is configured. Indeed, a certain degree of radiality in propagation (i.e. increased dispersion front) is expected, although the dispersion will occur mainly roughly perpendicular to the shore, especially for distributed sources such as multiple river mouths along a shore. A practical intermediate solution might be to adopt a decay function with doubled decay rate with respect to the case of parallel flow. This assumption is still conservative with respect to the radial case.

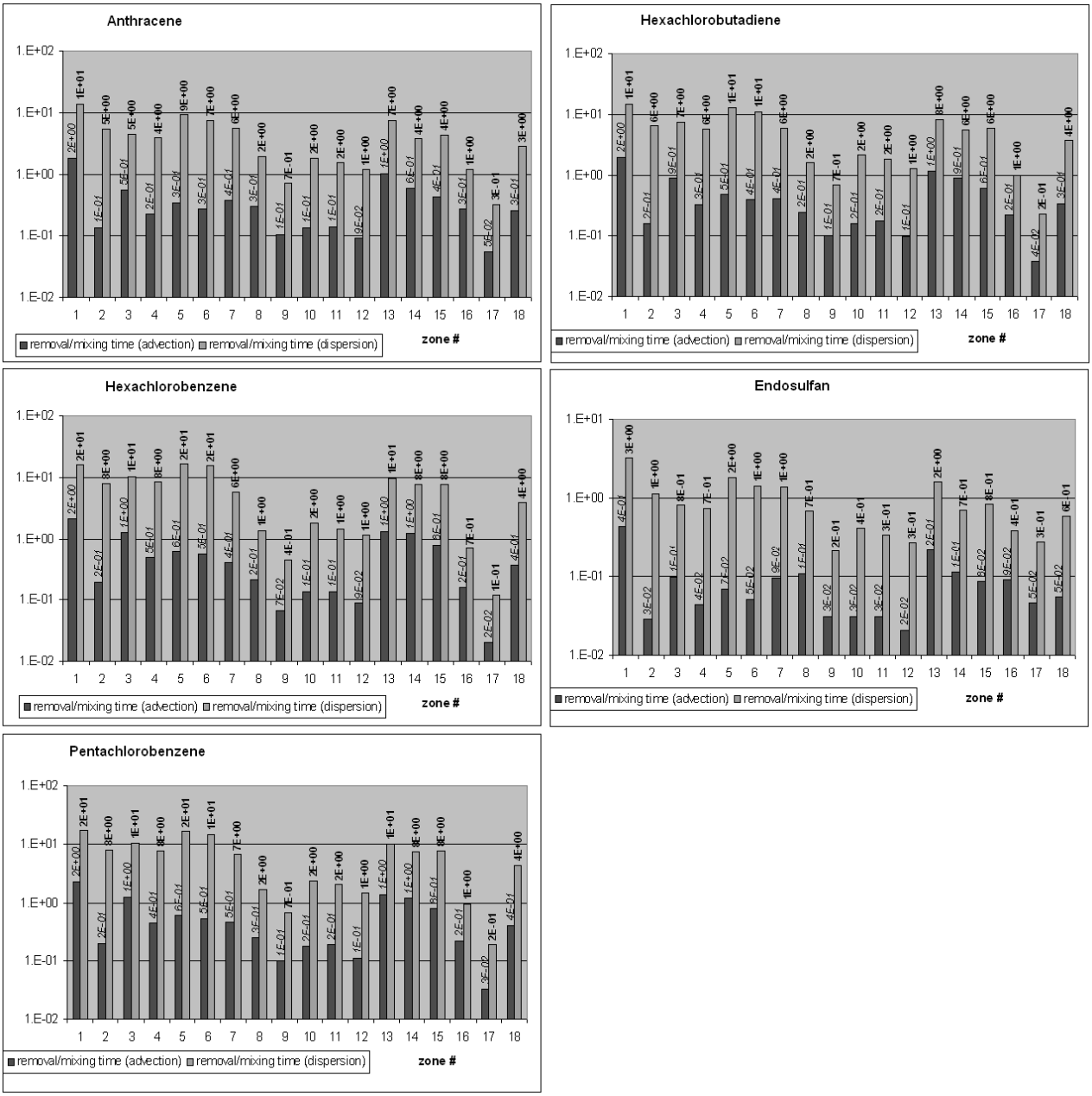

Figure 6 – Removal vs mixing time for the 5 chemicals of Table 3.

When advection is present, a steady state solution to the ADRE for parallel flow is a negative exponential with decay rate $\left[\sqrt{\left(\frac{v}{2D}\right)^2+\frac{k}{D}}\right]$. The parallel flow model is not appropriate when the emission occurs over a limited stretch of the coast having length L, so that it cannot be considered uniform. In such cases, there is a two-dimensional solution that can be written for the centerline of the dispersion plume as (e.g. . [55], p 485):

$$\frac{C(r)}{C(0)} = \exp\left(-\frac{k}{v}r\right) erf\left(\sqrt{\frac{vL^2}{16Dr}}\right). \qquad (11)$$

A practical intermediate solution might be again to adopt a decay function given by:

$$\frac{C(r)}{C(0)} = \exp\left(-2\left[\sqrt{\left(\frac{v}{2D}\right)^2+\frac{k}{D}}\right]r\right) \qquad (12)$$

which means doubled decay rate with respect to the case of parallel flow, exactly as in the case of dispersion only. When v=0 in Equation (13) we obtain the case of pure dispersion, consistently. When k=0 (no degradation) the second term of the decay rate disappears. Although the model can be only applied to idealized conditions with reference to a given advection direction, Equation (13) can be used to define an indicator of chemical concentration persistence from coastal areas, as:

$$I_i(x,y) = \exp\left(-2 \int_{L(x,y)} \sqrt{\left(\frac{v(\sigma)}{2D(\sigma)} \right)^2 + \frac{k(\sigma)}{D(\sigma)}} d\sigma \right) \qquad (13)$$

where the line integral is evaluated along the shortest pathway L(x,y) from the source to location (x,y), using the standard geographic information system (GIS) function known as cost distance [6], with parameters D, v and k used to compute the cost map $\sqrt{\left(\frac{v}{2D} \right)^2 + \frac{k}{D}}$. This indicator assumes that advection is always perpendicular to the coast, and represents the maximum seaward propagation of coastal pollution.

3. Results

3.1 Impact of the lateral exchange between zones on chemical mass distribution

We used the model to estimate the distribution of a chemical from given emissions. Two scenarios were deemed of particular interest: (1) unit emission per square km of surface all over European seas ("uniform emissions"), and (2) a unit emission in one at a time out of the 18 sea zones ("point emissions"). While for point emissions the mass in the cell computed is practically the same that would result from a water column calculation, i.e. M = E / (Kremoval + Ktransport), for uniform emissions the water column calculation may introduce underestimation when neglecting important contributions from surrounding zones. The ratio of mass obtained from the water column calculation, over mass obtained from the solution of the system (1), is an indicator of the "autonomy" of each zone. The closer the ratio to 100%, the less the zone is influenced by other connected zones. It is also of interest to evaluate the importance of lateral exchange over removal in the build up of mass in each zone. This can be assessed by comparing the mass resulting from the solution of the system (1) with the mass at steady state determined by "vertical" removal processes only (M = E / Kremoval). For uniform emissions, neglecting lateral exchanges may induce over- or under-estimation of mass in a sea zone, depending on whether a zone tends to be an "importer" or an "exporter" of chemicals, i.e. whether the emission to the cell is less or more important than the advective and dispersive fluxes coming from surrounding cells. For point emissions, neglecting lateral exchanges would lead to an overestimation of mass in the cell of emission. By taking the ratio of the total mass in a cell with lateral exchanges, over the mass without lateral exchanges, we obtain indicators of the "columnarity" or "self-containedness" of each zone. "Autonomy" and "columnarity" of the sea zones are conceptually correlated, but the former relates to the influence of external sources to each zone, whereas the latter refers to the importance of lateral over vertical processes within each zone. The above defined indicators are plotted in Figure 7 and Figure 8 for the chemicals of Table 3. Both autonomy and columnarity depend in principle on the chemical under consideration, and not just on environmental properties. From the graphs, however, it is apparent that the behaviour is rather similar among the different chemicals. For this reason, it makes sense to refer to the average for discussion. Autonomy of cells 14 and 15 is low (<50%), whereas the one of cells 1, 3, 4, 13, 16 is lower that 80%. This indicates that, when modeling rather homogeneous emissions, these zones should not be considered without the contribution from surrounding zones. Columnarity under uniform emissions reflects both the relevance of lateral transport over removal processes, and the effects of mass gradients across zones, whereas under point emission only the relevance of lateral transport over

removal. Under point emissions, zones 1, 4, 13, 14, 15 have a columnarity <50%, while zones 3, 5, 6, 8, 11, 12, 16, 18 have columnarity <80%. This indicates that all these zones should not be treated as independent water columns, i.e., when a local emission occurs, lateral advection and dispersion should be included. However, when considering uniform emissions, only zones 1 and 4 have columnarity <50%, while zones 5, 6, 8, 13, 18 have columnarity <80%. This indicates that, when emissions are rather uniformly distributed, the assumption of independent water columns holds for a wider share of European seas.

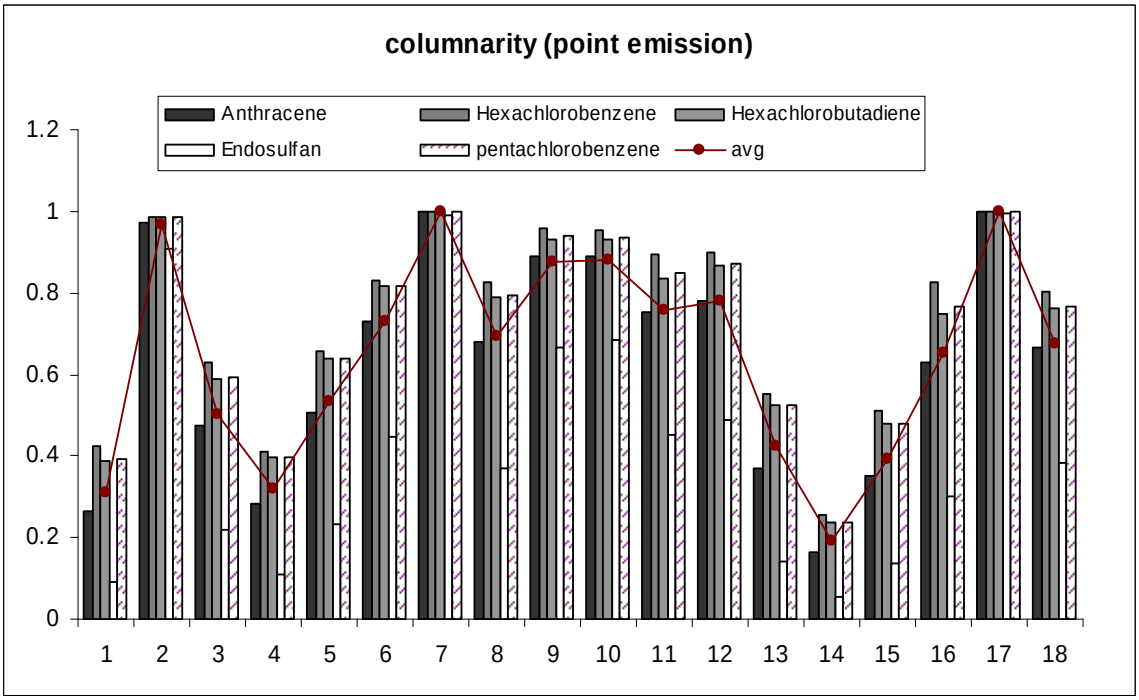

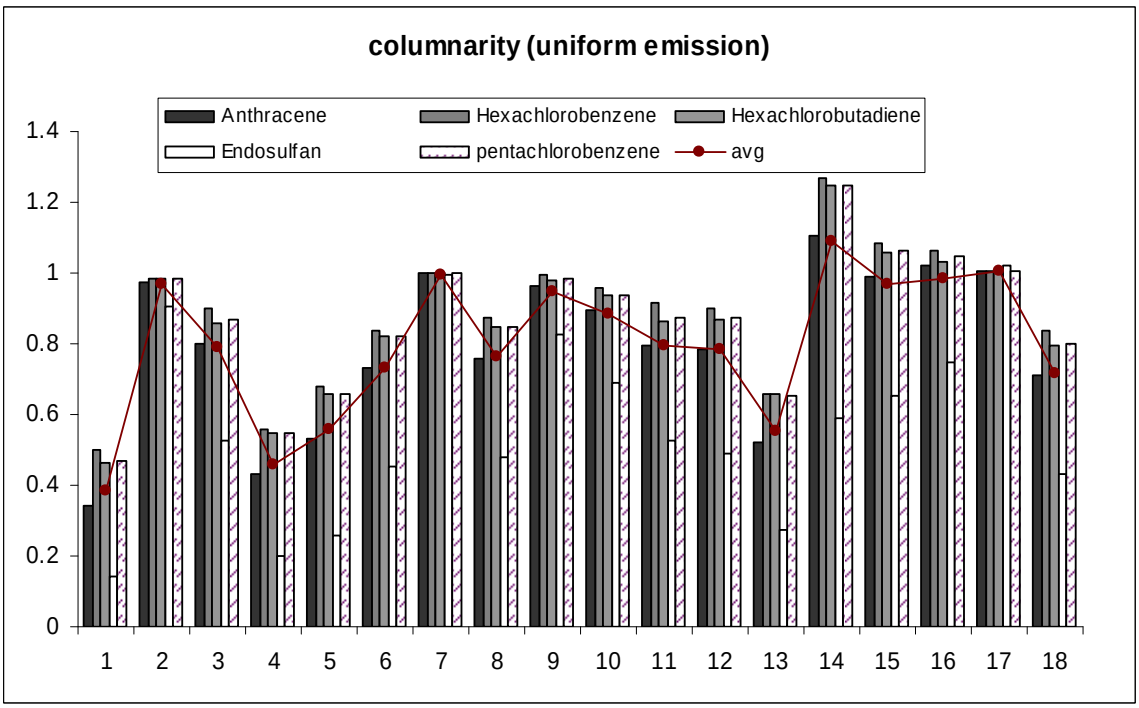

Figure 7 – Indicator of columnarity for each zone.

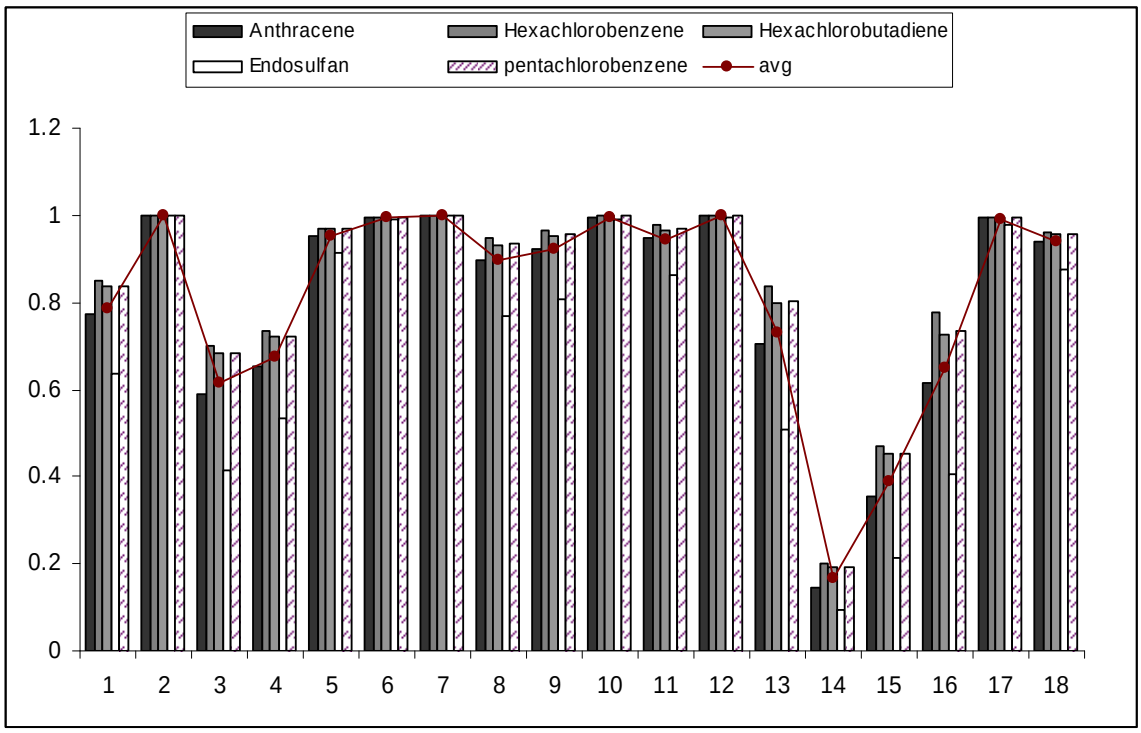

Figure 8 – Indicator of autonomy of each zone.

3.2 Mapping potential pollution from coastal sources

We used equation (13) to estimate the attenuation of concentrations from coastal zones to the seawater. In particular, we computed a map of I(x,y) for k=0 (conservative contaminant), as shown in Figure 9. We denote this specific map of I as $I_0(x,y)$.

The map highlights areas where attenuation due to dispersion and advection only play a more important role. These areas correspond to zones which are more difficult to reach, due to limited efficiency of the transport mechanisms. Examples include the inner part of the North Sea, and parts of the Mediterranean. The Black Sea appears to be divided in two distinct zones which correspond to the circulation pattern. However, most of the European seas are expected to have concentrations within a factor of 10 lower than in the coastal area. By computing I(x,y) for an arbitrary value of k, one may estimate the time of travel of contaminants in seawater $T = \frac{\ln\left(\frac{I_0(x,y)}{I(x,y)}\right)}{k}$, as shown in Figure 9. This method has been followed in the context of atmospheric transport modeling to provide a map of atmospheric time of travel [46, 47]. This way of estimating the time of travel is not sensitive to the value of k, as illustrated in Annex 1 - Sensitivity analysis. The joint use of I_0 and the time of travel map allows estimating I for an arbitrary non-conservative contaminant as $I=I_0\exp(-k\ T)$, thus simplifying calculations.

The time of travel provides also a guidance about the possibility to neglect degradation in chemical transport studies: if α is the maximum ratio we can accept between the normalized concentration I_0 of the conservative substance, and the normalized concentration I of a non-conservative substance, the substance with the maximum degradation rate that can be described under conservative assumptions corresponds to the rate $k(\alpha) = \ln(\alpha)/T$.

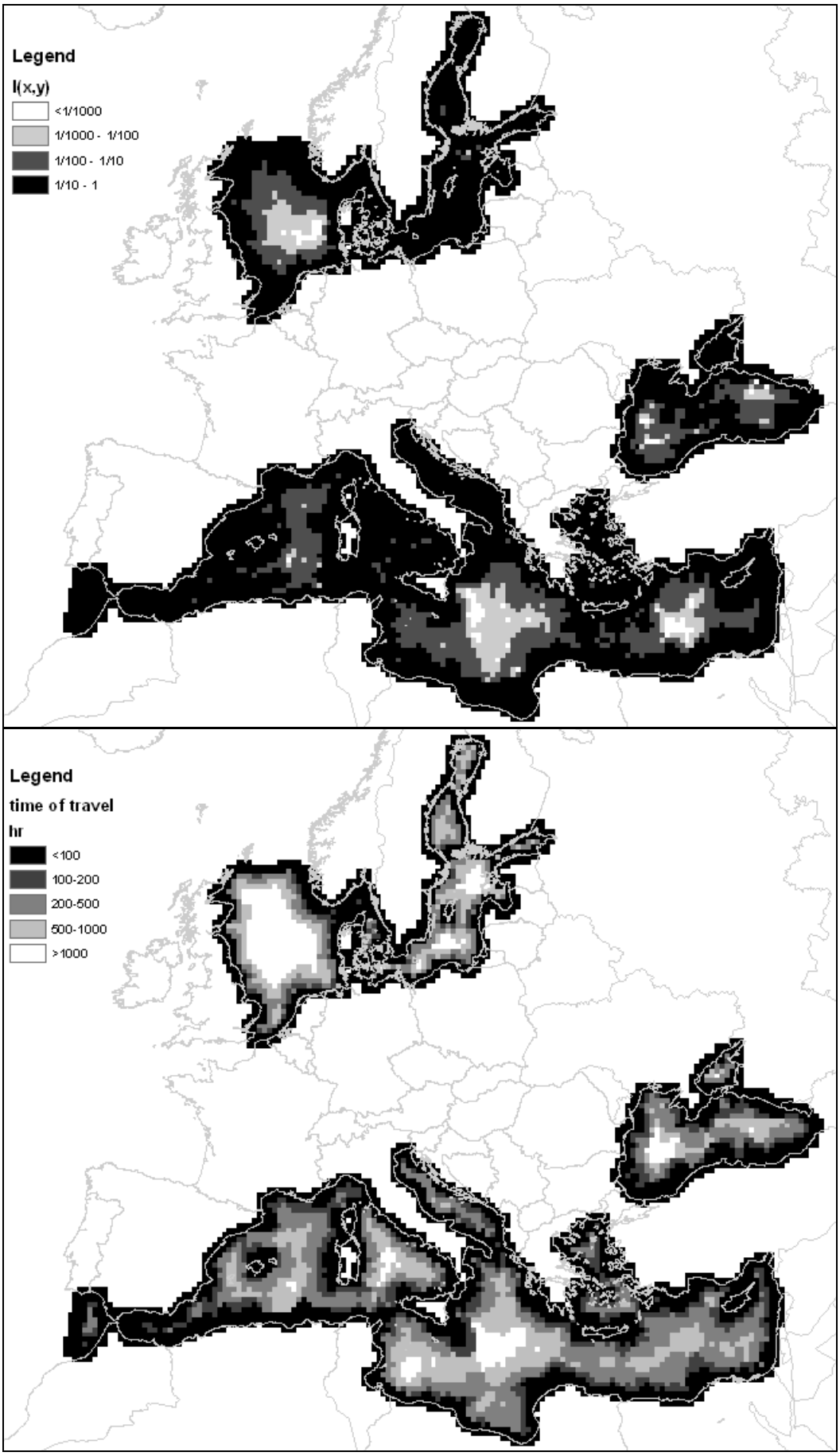

Figure 9 –Above: ratio of concentration in seawater versus concentration in the coastal zone. Below: Time of travel of contaminants from the coastal zone.

3.3 Discussion and conclusions

The patterns of seawater circulation, derived from a hydrodynamic model for European seas, allow identifying zones which correspond to gyres or to still water areas, with the exception of a few areas where a dominant advection direction can be identified. These zones can be looked at as homogeneous boxes and described as a system of CSTRs. This represents a simple scheme that can be used for the quantitative assessment of pollutants at a paneuropean scale. We use a corresponding system of mass balance equations to assess the relative importance of lateral transport and exchanges between zones, and vertical processes including settling of particles, volatilization and degradation. We show that in some cases the error introduced by neglecting lateral exchanges may be low (case of highly "autonomous" or "columnar" areas) due to low influence of external contributions, low importance of lateral transport from the zone outwards, or low mass gradients in space. In such cases, a "water column" approach to the modeling of pollutants can be adopted which greatly simplifies calculations. In other circumstances, however, interactions between zones should not be neglected.
Moreover, the spatial distribution of velocity and dispersion coefficient values used to parameterize the multiple box scheme presented in the report allows the estimation of spatially distributed parameters for simple plume models, which can be used to map the attenuation of coastal pollution seawards. For demonstration, we build a map of contamination attenuation for a conservative chemical, and a map of time of travel, which can be combined to describe a generic non-conservative chemical.
A comprehensive seawater circulation and contaminant transport model remains the elective tool for the simulation of pollution. However, under conditions of high uncertainty and for screening level purposes, preliminary calculations can be conducted using simplified tools. When appropriate, a water column approach has been already demonstrated to be useful for the understanding of processes. We suggest that using circulation patterns from more comprehensive models to parameterize simple models, such as plume and multiple-box models, be as valuable a tool when water column approaches cannot be accepted. Future lines of research should include an experimental evaluation of the proposed models.

4. Acknowledgements and software available

Colleagues Frederic Melin and David Pennington from EC, DG JRC are gratefully acknowledged for helpful discussion. Frederic Melin also provided the estimates of TSM that were processed for this study. A MS Excel © implementation of the multiple box model proposed here is made available for further research (contact Authors for a copy). The model contains a specific worksheet displaying the source-receptor relationships for the zones thereby identified. Data about PFOS and PFOA concentrations used in Annex 2 were compiled by colleague Robert Loos of the JRC (contact the Authors for further information and availability of the dataset).

5. References

1. A. A. Androsov, B. A. Kagan, D. A. Romanenkov and N. E. Voltzinger, Numerical modelling of barotropic tidal dynamics in the strait of Messina, Advances in Water Resources, Volume 25, Issue 4, April 2002, Pages 401-415.
2. A. Stips, K. Bolding, T. Pohlman, and H. Burchard, "Simulating the temporal and spatial dynamics of the North Sea using the new model GETM (General Estuarine Transport Model)," Ocean Dynamics, vol. 54, pp. 266-283, 2004.
3. A.Gusev, E.Mantseva, V.Shatalov, B.Strukov , EMEP/MSC-E Technical Report 5/2005 "Regional Multicompartment Model MSCE-POP"
4. *Brandes, L.J., den Hollander, H., van de Meent, D., Simplebox 2.0: a nested multimedia fate model for evaluating the environmental fate of chemicals, RIVM Report no. 719101029, Bilthoven, december 1996*
5. Burchard, H., Bolding, K., GETM: a general estuarine transport model. Scientific documentation. Tech.Rep. EUR 20253, Ispra, 2002

6. Burrough, P.A., Mc Donnel, R., Principles of Geographical Information Systems. Oxford University Press, 1998
7. Csanady, G.T., Turbulent diffusion in the environment, Reidel, Dordrecht, 1973, 248 pp
8. Dachs, J., Bayona, J., Raoux, C., Albaiges, J., Spatial, Vertical Distribution and Budget of Polycyclic Aromatic Hydrocarbons in the Western Mediterranean Seawater, Environ.Sci.Technol., 1997, 31, 682-688
9. Dachs, j., Lohmann, R., Ockenden, W., Mejanelle, L., Eisenreich, S.J., Jones, K.C., Oceanic biogeochemical controls on global dynamics of POPs, Environ.Sci.Technol., 2002, 36: 4229-4237
10. Directive 2000/60/EC of the European Parliament and of the Council of 23 October 2000, establishing a framework for community action in the field of water policy.
11. E. V. Stanev, G. Brink-Spalink, and J.-O. Wolff, "Sediment dynamics in tidally dominated environments controlled by transport and turbulence. A case study for the East Frisian Wadden Sea," *J. Geophys. Res.*, 2007, 112, C04018.
12. Fernando Gomez, The role of the exchanges through the Strait of Gibraltar on the budget of elements in the Western Mediterranean Sea: consequences of human-induced modifications, Marine Pollution Bulletin, Volume 46, Issue 6, June 2003, Pages 685-694.
13. Garcia-Gorriz, E., Stips, A., Report on the first results from the Mediterranean Sea model. Report EUR 22141 EN, Ispra 2006.
14. Gusev, A., Mantseva, E., Rozovskaya, O., Shatalov, V., Strukov. B., Vulykh, N., Aas, W., Breivik, K., Persistent Organic Pollutants in the Environment, EMEP status report 3/2005, june 2005 (www.emep.int)
15. Jurado, E., Jaward, F.M., Lohmann, R., Jones, K.C., Simo', R., Dachs, J., Atmospheric Dry deposition of POPs to the Atlantic and inferences for the global oceans, Environ.Sci.Technol., 2004, 38: 5505-5513
16. Jurado, E., Jaward, F.M., Lohmann, R., Jones, K.C., Simo', R., Dachs, J., Wet deposition of POPs to the global oceans, Environ.Sci.Technol., 2005, 39: 2426-2435
17. Jurado, E., Zaldívar, J., Marinov, D., Dachs, J., Fate of persistent organic pollutants in the water column: Does turbulent mixing matter? Marine Pollution Bulletin, Volume 54, Issue 4, April 2007, Pages 441-451
18. K.J. Curran, P.S. Hill, T.G. Milligan, O.A. Mikkelsen, B.A. Law, X. Durrieu de Madron, F. Bourrin, Settling velocity, effective density, and mass composition of suspended sediment in a coastal bottom boundary layer, Gulf of Lions, France, Continental Shelf Research 27 (2007) 1408–1421
19. Kamburska, L., personal communication, 2006.
20. Krishnaswami, S., Sarin, M., Atlantic surface particulates: composition, settling rates and dissolution in the Deep sea, Earth and Planetary Science Letters, 32, pp 430-440, 1976
21. L. Toose, D.G. Woodfine, M. MacLeod, D. Mackay, J. Gouin, BETR-World: a geographically explicit model of chemical fate: application to transport of a-HCH to the Arctic, Environmental Pollution 128 (2004) 223–240
22. Mackay, D., Multimedia Environmental models: the fugacity approach, 2nd ed., Lewis Publishers, New York, 2001, 261 pp
23. Mackay, D., Paterson, S., Kicsi, G., Di Guardo, A., Cowan, C.E., Assessing the fate of new and existing chemicals: a five-stage process, Env. Tox. Chemistry, 15(9):1618-1626, 1996
24. Mackay, D., Shiu, W.Y., Ma, K.C., Illustrated handbook of physico-chemical properties and environmental fate for organic chemicals. Vol. V, pesticide chemicals. Lewis/CRC Press, , New York, 1997
25. MacLeod, M., Woodfine, D.G., Mackay, D., McKone, T., Bennet, D., Maddalena, R., 2001. BETR North America: a regionally segmented multimedia contaminant fate model for North America. Environmental Science and Pollution Research 8 (3), 156–163.
26. Mariano, A.J., E.H. Ryan, B.D. Perkins and S.Smithers, 1995: The Mariano Global Surface Velocity Analysis 1.0. USCG Report CG-D-34-95, 55 pp

27. Mc Cave, N., Vertical flux of particles in the Ocean, Deep sea research, vol 22, pp491-502, 1975
28. Mélin, F., C. Steinich, N. Gobron, B. Pinty, M.M. Verstraete: "Optimal merging of LAC and GAC data from SeaWiFS." Int. J. Remote Sens., 23, 801-807, 2002.
29. Mélin, F., G. Zibordi, J.-F. Berthon: "Assessment of SeaWiFS atmospheric and marine products for the Northern Adriatic Sea." IEEE Trans. Geosci. Remote Sens., 41, 548-558, 2003.
30. Menesguen, A., Cugier, P., Loyer, S., Vanhoutte-Brunier, A., Hoch, T., Guillaud, J. , Gohin, F., Two- or three-layered box-models versus fine 3D models for coastal ecological modelling? A comparative study in the English Channel (Western Europe), Journal of Marine Systems, Volume 64, Issues 1-4, Contributions from Advances in Marine Ecosystem Modelling Research, 27-29 June, 2005, Plymouth, UK, AMEMR, January 2007, Pages 47-65.
31. Michel,P., Averty, B., Distribution and Fate of Tributyltin in Surface and Deep Waters of the Northwestern Mediterranean, Environ.Sci.Technol.1999, 33, 2524-2528
32. Monterey, G. and Levitus, S., 1997: Seasonal Variability of Mixed Layer Depth for the World Ocean. NOAA Atlas NESDIS 14, U.S. Gov. Printing Office, Washington D.C., 96 pp. 87 figs.
33. N. S. Banas and B. M. Hickey, "Mapping exchange and residence time in a model of Willapa Bay, Washington, a branching, macrotidal estuary," *J. Geophys. Res.*, vol. 110, p. C11011, 2005.
34. Noh, Y., Kang, I.S., Herold, M., Raasch, S., Large eddy simulation of particle settling in the ocean mixed layer, physics of fluids, 18, 085109, 2006
35. Noriyuki Suzuki, Kaori Murasawa, Takeo Sakurai, Keisuke Nansai, Keisuke Matsuhashi, Yuichi Moriguchi, Kiyoshi Tanabe, Osami Nakasugi, and Masatoshi Morita, Geo-Referenced Multimedia Environmental Fate Model (G-CIEMS): Model Formulation and Comparison to the Generic Model and Monitoring Approaches *Environ. Sci. Technol.,* **38** (21), 5682 -5693, 2004
36. Okubo, A., Oceanic diffusion diagrams, Deep sea research, vol 18, pp789-802, 1971
37. Peneva, E., Stips, A., Numerical simulations of the Black Sea and adjoined Azov sea, forced with climatological and meteorological reanalysis data. Report EUR 21504 EN, Ispra, 2005
38. Pennington, D.W., M. Margni, C. Amman and O. Jolliet, 2005. Multimedia fate and human intake modeling: spatial versus nonspatial insights for chemical emissions in Western Europe. Environmental Science and Technology 39: 1119-1128
39. Pistocchi, A. (2008). A GIS-based approach for modeling the fate and transport of pollutants in Europe , Environmental Science and Technology, 42, 3640-3647.
40. Pistocchi, A. (2008) Fate and Transport models. In Encyclopedia of Quantitative Risk Assessment and Analysis – Melnick, E., Everitt, B. (eds), John Wiley and Sons, Chichester, UK, pp 705-714.
41. Pistocchi, A., Galmarini, S., Evaluation of a Simple Spatially Explicit Model of Atmospheric Transport of Pollutants in Europe; in press, Environmental Modeling and Assessment, 2009. DOI: 10.1007/s10666-008-9187-x
42. Pistocchi, A., Vizcaino Martinez, M.P., Pennington, D.W., Analysis of Landscape and Climate Parameters for Continental Scale Assessment of the Fate of Pollutants; Luxembourg: Office for Official Publications of the European Communities, EUR 22624 EN, 108 pp., 2006
43. Prevedouros, K., M. McLeod, K.C. Jones and A.J. Sweetman, 2004. Modelling the fate of persistent organic pollutants in Europe: parameterization of a gridded distribution model. Environmental Pollu-tion 128: 251-261
44. Rajar , R., M. Četina, M.Horvat, D.Žagar, Mass balance of mercury in the Mediterranean Sea, Marine Chemistry xx (2006) xxx–xxx In press
45. Richards, K.J., Jia, Y., Rogers, C.F., Dispersion of tracers by ocean gyres, Journal of physical oceanography, vol. 25, pp 874-887, 1995
46. Roemer, M., Baart, A., Libre, J.M., ADEPT: development of an Atmospheric Deposition and Transport model for risk assessment, TNO report B&O- A R 2005-208, Apeldoorn, 2005

47. Schwarzenbach, R. P.; Gschwend, P. M.; Imboden, D. M. Environmental Organic Chemistry; Wiley: New York, 1993
48. Sentchev, A., Max Yaremchuk and Florent Lyard, Residual circulation in the English Channel as a dynamically consistent synthesis of shore-based observations of sea level and currents, Continental Shelf Research, Volume 26, Issue 16, October 2006, Pages 1884-1904.
49. Slutz, R.J., S.J. Lubker, J.D. Hiscox, S.D. Woodruff, R.L. Jenne, D.H. Joseph, P.M. Steurer, and J.D. Elms, 1985, *Comprehensive Ocean-Atmosphere Data Set; Release 1.* NOAA Environmental Research Laboratories, Climate Research Program, Boulder, CO, 268 pp. (NTIS PB86-105723).
50. Smagorinsky, J., General circulation experiments with the primitive equations, I.The basic experiment. Monthly weather review, vol. 91, n. 3, pp 99-152, march 1963
51. Stanev, E., Understanding Black Sea Dynamics. An overview of Recent Numerical Modeling, Oceanography, vol. 18, no. 2, pp 56-75, 2005.
52. Stips, A., Bolding, K., Burchard, H., Djavidnia, S., Peneva, E., Realistic Multiannual simulations of the coupled North Sea and Baltic Sea system using the GETM model. Report EUR 21503 EN, Ispra, 2005
53. T. Ilyina, T. Pohlmann, G. Lammel and J. Sundermann, A fate and transport ocean model for persistent organic pollutants and its application to the North Sea, Journal of Marine Systems, Volume 63, Issues 1-2, November 2006, Pages 1-19
54. Tang, C.L., D'Alessio S.J.D., De Tracey, B.M., Mixed-layer simulations at OWS Bravo: the role of salinity in interannual variability of the upper ocean at high latitude. International Journal of Oceans and Oceanography ISSN 0973-2667 Vol.1 No.1, pp. 119-139, 2006.
55. Thibodeaux, L., Environmental Chemodynamics, 2nd ed., Wiley, New York, 1996, 593 pp
56. Wania, F., D. Mackay 1995. A global distribution model for persistent organic chemicals. Sci. Total Environ. 160/161: 211-232
57. Weigel, Stefan, Jan Kuhlmann, Heinrich Huehnerfuss, Drugs and personal care products as ubiquitous pollutants: occurrence and distribution of clofibric acid, caffeine and DEET in the North Sea, The Science of the Total Environment, 295, 131-141, 2002
58. Wheatcraft, S.W., Travel time equations for dispersive contaminants, Groundwater, 38:4, pp. 505-509, 2000
59. Zaldívar, J.M., Lars Håkanson, Naiara Berrojalbiz, Sibylle Dueri, Roberta Carafa , Dimitar Marinov, Elena Jurado and Jordi Dachs, The Use Of Models For Ecological Risk Assessment In Coastal Ecosystems: Thresholds Point Of View . EUR 22269 EN – DG Joint Research Centre, Institute for Environment and SustainabilityLuxembourg: Office for Official Publications of the European Communities, 2006 – 50pp.
60. Holte, T.J., L. Talley, A New Algorithm for Finding Mixed Layer Depths with Appplications to ARGO data and Subantarctic Mode Water Formation, J. Atm. Oceanic Technologies, Vol. 26, 1921-1939, 2009.

6. Annex 1 – Sensitivity analysis

The results of a sensitivity analysis with respect to organic carbon content of TSM and settling velocity are provided hereafter. For the 5 chemicals of Table 3, the total removal rate (degradation +volatilization + settling) was computed in the baseline case (organic carbon =0.5% of TSM and settling velocity $v=10^{-4}$ m/s) and, while keeping one of the two parameters, the other was varied (organic carbon between 25% and 75%, settling velocity between 10^{-3} and 10^{-5} m/s). The graphs in Figure 10 show the results, indicating that the removal rate is relatively insensitive to these parameters in the case of the 5 chemicals analyzed. For less hydrophobic and/or more persistent chemicals (e.g. perfluorinated compounds), the picture may be slightly different

In order to test the sensitivity of the time of travel (see section 0) to the choice of a reference value of the removal rate k, we generated a field of random values of velocity and dispersion coefficients as a function of distance, and we computed the ratio C(r)/C(0) according to equation (12), under the case of parallel flow. An example of the calculation (i.e. one single random field realization) is shown in Table 4. The random fields were generated in Excel using the RND() function, with the statistics of Table 5, according to the formula: $X^*= \min(\max(X), \max(\min(X), X + RND() * X_{stdev} - RND()*X_{stdev}))$, where X* is the generated random value (X=v or X=D), min(X) and max(X) are its minimum and maximum statistics, X_{avg} and X_{stdev} the mean and standard deviation. Example results are shown in Figure 11. By running several random generations, it was possible to verify that the sensitivity of the time of travel to the value taken for k was rather limited, especially at low distances (less than 300 km from the coast). The graphs of Figure 11 are representative of this situation.

A- distance km	*B- v (m/s)*	*C- D(m2/s)*	*D- C/C_0 no decay*	*E- C/C_0 k=0.0001*	*F- C/C_0 k=0.001*	*G-- C/C_0 k=0.00001*	*H- C/C_0 T.t., k=0.0001*	*I- C/C_0 T.t., k=0.001*	*J- C/C_0 T.t., k=0.00001*
2.5E+01	7.7E-02	1.4E+03	5.1E-01	5.0E-01	4.6E-01	5.0E-01	9.0E+01	8.5E+01	9.1E+01
5.0E+01	7.5E-02	1.5E+03	2.8E-01	2.7E-01	2.3E-01	2.8E-01	1.8E+02	1.7E+02	1.8E+02
7.5E+01	1.2E-01	1.2E+03	8.0E-02	7.8E-02	6.4E-02	8.0E-02	2.4E+02	2.3E+02	2.4E+02
1.0E+02	8.9E-02	1.7E+03	4.2E-02	4.0E-02	3.1E-02	4.2E-02	3.2E+02	3.0E+02	3.2E+02
1.3E+02	1.3E-01	2.5E+03	2.2E-02	2.1E-02	1.6E-02	2.2E-02	3.7E+02	3.5E+02	3.7E+02
1.5E+02	1.3E-01	2.0E+03	9.5E-03	9.1E-03	6.3E-03	9.4E-03	4.2E+02	4.1E+02	4.3E+02
1.8E+02	1.1E-01	2.0E+03	4.8E-03	4.6E-03	3.0E-03	4.8E-03	4.9E+02	4.6E+02	4.9E+02
2.0E+02	8.1E-02	1.5E+03	2.5E-03	2.3E-03	1.4E-03	2.5E-03	5.7E+02	5.5E+02	5.7E+02
2.3E+02	5.7E-02	1.9E+03	1.7E-03	1.6E-03	8.8E-04	1.7E-03	6.9E+02	6.5E+02	7.0E+02
2.5E+02	5.9E-02	2.9E+03	1.3E-03	1.2E-03	6.2E-04	1.3E-03	8.1E+02	7.5E+02	8.1E+02
2.8E+02	3.7E-02	2.6E+03	1.1E-03	9.9E-04	4.5E-04	1.1E-03	9.8E+02	8.9E+02	1.0E+03
3.0E+02	4.7E-02	1.2E+03	6.8E-04	6.1E-04	2.5E-04	6.7E-04	1.1E+03	1.0E+03	1.1E+03
3.3E+02	3.1E-02	3.0E+03	6.0E-04	5.2E-04	1.9E-04	5.9E-04	1.3E+03	1.2E+03	1.4E+03
3.5E+02	6.0E-02	2.3E+03	4.3E-04	3.7E-04	1.2E-04	4.3E-04	1.4E+03	1.3E+03	1.5E+03
3.8E+02	1.1E-01	2.1E+03	2.2E-04	1.9E-04	6.0E-05	2.2E-04	1.5E+03	1.3E+03	1.5E+03
4.0E+02	9.6E-02	1.8E+03	1.2E-04	9.9E-05	2.9E-05	1.1E-04	1.6E+03	1.4E+03	1.6E+03
4.3E+02	3.0E-02	1.2E+03	8.4E-05	7.0E-05	1.8E-05	8.3E-05	1.8E+03	1.6E+03	1.8E+03
4.5E+02	7.6E-02	7.5E+02	2.4E-05	2.0E-05	4.6E-06	2.4E-05	1.9E+03	1.7E+03	1.9E+03
4.8E+02	7.0E-02	2.6E+02	8.1E-07	6.7E-07	1.4E-07	8.0E-07	2.0E+03	1.8E+03	2.0E+03
5.0E+02	7.0E-02	2.8E+03	5.9E-07	4.8E-07	9.4E-08	5.8E-07	2.1E+03	1.8E+03	2.1E+03
5.3E+02	3.8E-02	3.0E+03	5.0E-07	4.0E-07	7.0E-08	4.9E-07	2.3E+03	2.0E+03	2.3E+03
5.5E+02	8.1E-02	2.4E+03	3.3E-07	2.6E-07	4.3E-08	3.2E-07	2.4E+03	2.1E+03	2.4E+03
5.8E+02	8.6E-02	9.0E+02	1.0E-07	7.8E-08	1.2E-08	9.7E-08	2.4E+03	2.1E+03	2.5E+03
6.0E+02	5.5E-02	2.2E+03	7.3E-08	5.6E-08	7.8E-09	7.1E-08	2.6E+03	2.2E+03	2.6E+03
6.3E+02	3.4E-02	2.0E+03	5.9E-08	4.5E-08	5.4E-09	5.7E-08	2.8E+03	2.4E+03	2.8E+03
6.5E+02	1.2E-01	1.9E+03	2.7E-08	2.1E-08	2.4E-09	2.7E-08	2.8E+03	2.4E+03	2.9E+03
6.8E+02	6.1E-02	1.6E+03	1.7E-08	1.3E-08	1.3E-09	1.7E-08	2.9E+03	2.5E+03	3.0E+03
7.0E+02	9.4E-02	1.2E+03	6.3E-09	4.7E-09	4.6E-10	6.2E-09	3.0E+03	2.6E+03	3.1E+03
7.3E+02	1.0E-01	2.3E+03	3.6E-09	2.7E-09	2.5E-10	3.5E-09	3.1E+03	2.7E+03	3.1E+03
7.5E+02	9.7E-02	2.6E+03	2.2E-09	1.6E-09	1.4E-10	2.2E-09	3.1E+03	2.7E+03	3.2E+03
7.8E+02	8.8E-02	2.4E+03	1.4E-09	1.0E-09	8.4E-11	1.4E-09	3.2E+03	2.8E+03	3.3E+03
8.0E+02	1.3E-01	2.2E+03	6.7E-10	4.8E-10	3.8E-11	6.5E-10	3.3E+03	2.9E+03	3.3E+03
8.3E+02	1.3E-01	2.3E+03	3.4E-10	2.4E-10	1.8E-11	3.3E-10	3.3E+03	2.9E+03	3.4E+03
8.5E+02	1.2E-01	2.3E+03	1.7E-10	1.2E-10	8.8E-12	1.7E-10	3.4E+03	3.0E+03	3.4E+03
8.8E+02	8.3E-02	2.4E+03	1.1E-10	8.0E-11	5.3E-12	1.1E-10	3.5E+03	3.1E+03	3.5E+03
9.0E+02	5.8E-02	1.4E+03	6.8E-11	4.7E-11	2.9E-12	6.5E-11	3.6E+03	3.2E+03	3.6E+03
9.3E+02	7.3E-02	3.4E+03	5.2E-11	3.6E-11	2.0E-12	5.0E-11	3.7E+03	3.2E+03	3.7E+03
9.5E+02	4.5E-02	2.4E+03	4.1E-11	2.8E-11	1.4E-12	4.0E-11	3.8E+03	3.4E+03	3.9E+03
9.8E+02	1.1E-01	2.8E+03	2.5E-11	1.7E-11	8.2E-13	2.4E-11	3.9E+03	3.4E+03	4.0E+03
1.0E+03	7.6E-02	1.4E+03	1.3E-11	8.6E-12	3.8E-13	1.2E-11	4.0E+03	3.5E+03	4.0E+03

Table 4 - The ratio of concentration to initial concentration is plotted as a function of distance (column A) and different overall decay constants (cols D:G); velocity and dispersion coefficient are randomly generated within the bounds of the statistics of Table 5. Time of travel is computed accordingly (cols H:J)

	v	D
max	0.705907	0.000652
min	0	19421.26
mean	0.086662	1833.141
stdev	0.083523	1901.412

Table 5 – Statistics of velocity (v, m/s) and dispersion coefficient (D, m^2/s) used for the random field generation.

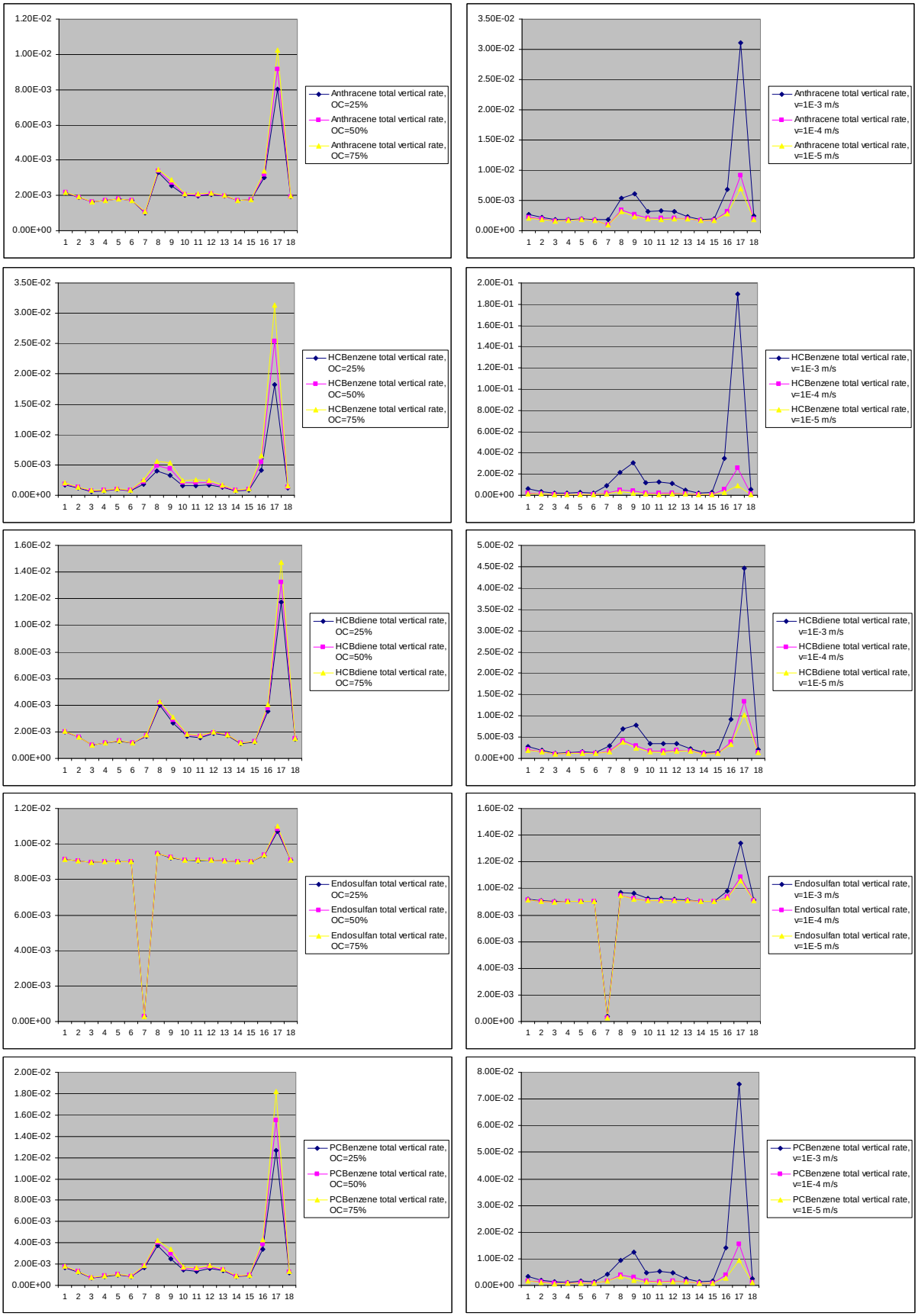

Figure 10 – Sensitivity analysis of the total removal rate to settling velocity (right column) and organic carbon content of the suspended sediments (left column). Rates on the y-axis are in hr-1; the numbers on the x-axis indicate the sea zone (see Figure 2).

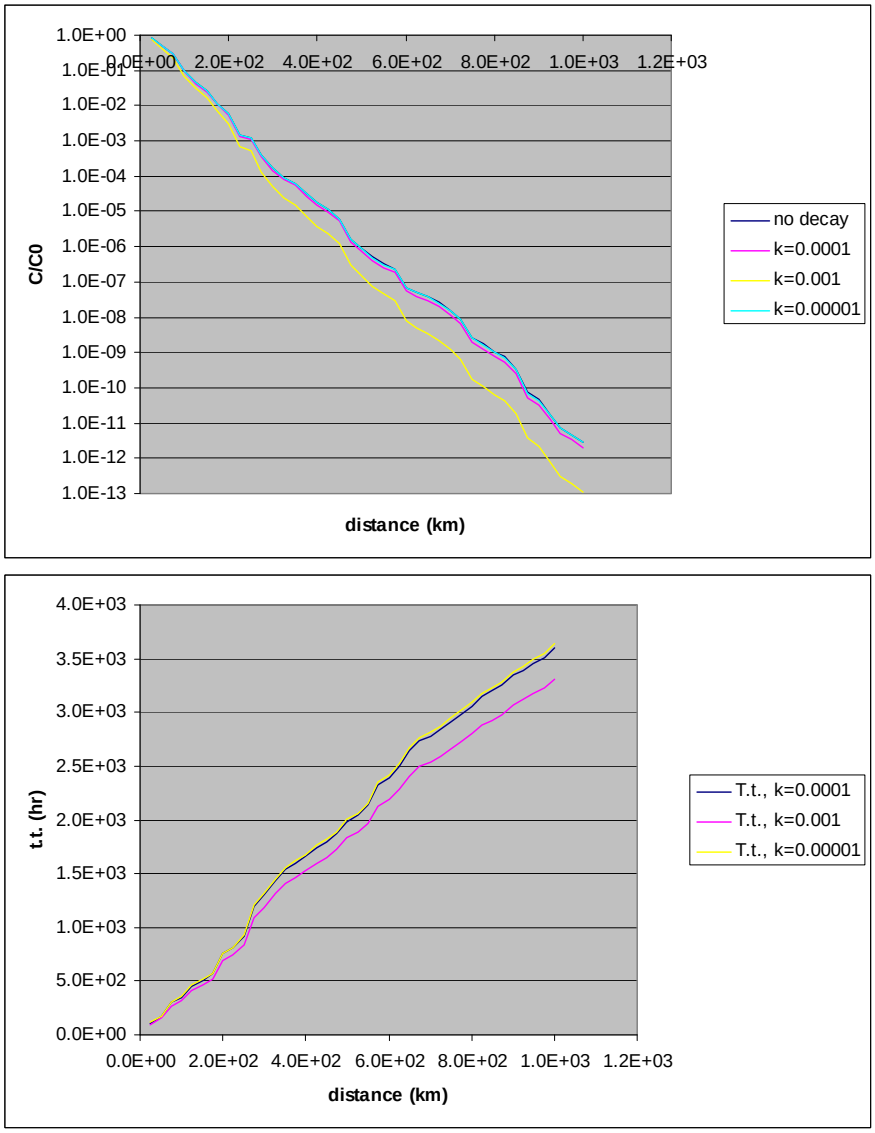

Figure 11 – Example graphs of the time of travel and C(r)/C(0) for different decay rates

7. Annex 2 – Some additional considerations on the exponential decay model for coastal pollution

We present a simple conceptual model for the spatial distribution of pollution from coastal sources. Conceptual models have been long and widely used in hydrology to build representations of phenomena, and consist in avoiding a realistic depiction of physical processes in favour of a largely simplified mechanistic scheme, of which the different parameters are obtained through pure mathematical and statistical calibration, although maintaining a link to measurable physical processes. In the domain of chemical fate and transport, linear box models can be regarded as conceptual models.
Conceptually, coastal waters contamination from a source having a finite size, small compared to the scale of contamination, can be described by the well known Gaussian plume model [see e.g.[7], p.105]:

$$C = \frac{1}{2} C_0 \left\{ erf\left(\frac{y+b}{\sqrt{2}\sigma}\right) - erf\left(\frac{y-b}{\sqrt{2}\sigma}\right) \right\}$$

where C represents concentration, C_0 its value at the coast, b the size of the source assumed orthogonal to the coast, y the distance orthogonal to the coast, and σ the plume dispersion, which is a function of y and the distance along the coast, x, in turn assumed parallel to the advective current.
By definition, the plume dispersion is related to the dispersion coefficient D by the following equation:

$$D = \frac{1}{2}\frac{d\sigma^2}{dt}, \text{ or}$$

$$\sigma^2 = \alpha + 2\int_0^t D d\tau$$

where α is an appropriate initial value of the dispersion. This can be chosen in practice as $\alpha = b^2$.
Moreover, assuming a constant velocity u along the x axis (parallel to the coast) we can write σ independent of time as:

$$\sigma^2 = b^2 + \frac{2D}{u} x .$$

Concentration becomes then:

$$C = \frac{1}{2} C_0 \left\{ erf\left(\frac{y+b}{\sqrt{2b^2 + \frac{4D}{u}x}}\right) - erf\left(\frac{y-b}{\sqrt{2b^2 + \frac{4D}{u}x}}\right) \right\}$$

If one assumes D proportional to a power of the plume length, or:

$$D = \gamma x^{\delta}$$

with γ, δ constant, concentration becomes:

$$C = \frac{1}{2} C_0 \left\{ erf\left(\frac{y+b}{\sqrt{2b^2 + \frac{4\gamma}{u\delta}x^{\delta+1}}}\right) - erf\left(\frac{y-b}{\sqrt{2b^2 + \frac{4\gamma}{u\delta}x^{\delta+1}}}\right) \right\}$$

Let's now consider a point (x,y) at the downstream end of a stretch of coast along which a number *n* emissions occur (x-axis), each one of intensity E_i (i=1 to n) and mixing width b orthogonal to the coast (y-axis); assume that the mixing depth h of coastal waters is also constant. Therefore, initial concentration at each emission location is $C_{0i} = E_i / b\ h\ u$.
The concentration for D depending on x can be expressed in such form as:

$$C = \frac{1}{2}\sum_{i=1}^{n} C_{0i}\left\{ erf\left(\frac{y+b}{\sqrt{2b^2 + \frac{4\gamma}{u\delta}(x-x_i)^{\delta+1}}}\right) - erf\left(\frac{y-b}{\sqrt{2b^2 + \frac{4\gamma}{u\delta}(x-x_i)^{\delta+1}}}\right)\right\}$$

where x_i is the abscissa of the i-th emission along the coast. A similar expression is obtained with constant D.

By superimposing the plumes from a high number of sources upstream based on the above formula, one obtains a profile of concentration as a function of the distance from the coast, at a given cross section, which follows with good approximation an exponential profile:

$$\frac{C(r)}{C(0)} = \exp\left(-\frac{v}{D}r\right)$$

which is equation (12) with k=0.

Examples of superimposition of 200 sources with different spacing upstream are shown in Figure 12 - Figure 15 (referred to the case of constant D and v, set to 1000 m^2/s and 0.05 m/s respectively). It is apparent that, when the spacing increases, the sum tends to the above equation. Results depend only on the v/D ratio.

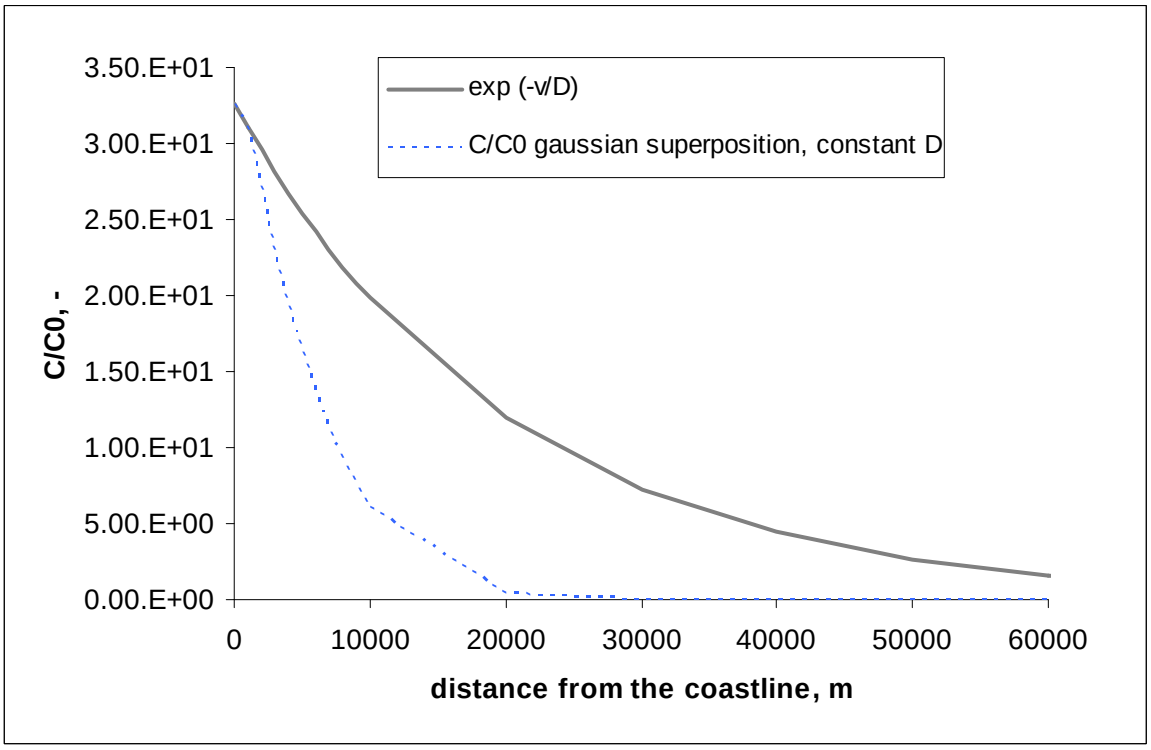

Figure 12 - Spacing 10 m, 200 emissions upstream (2 km)

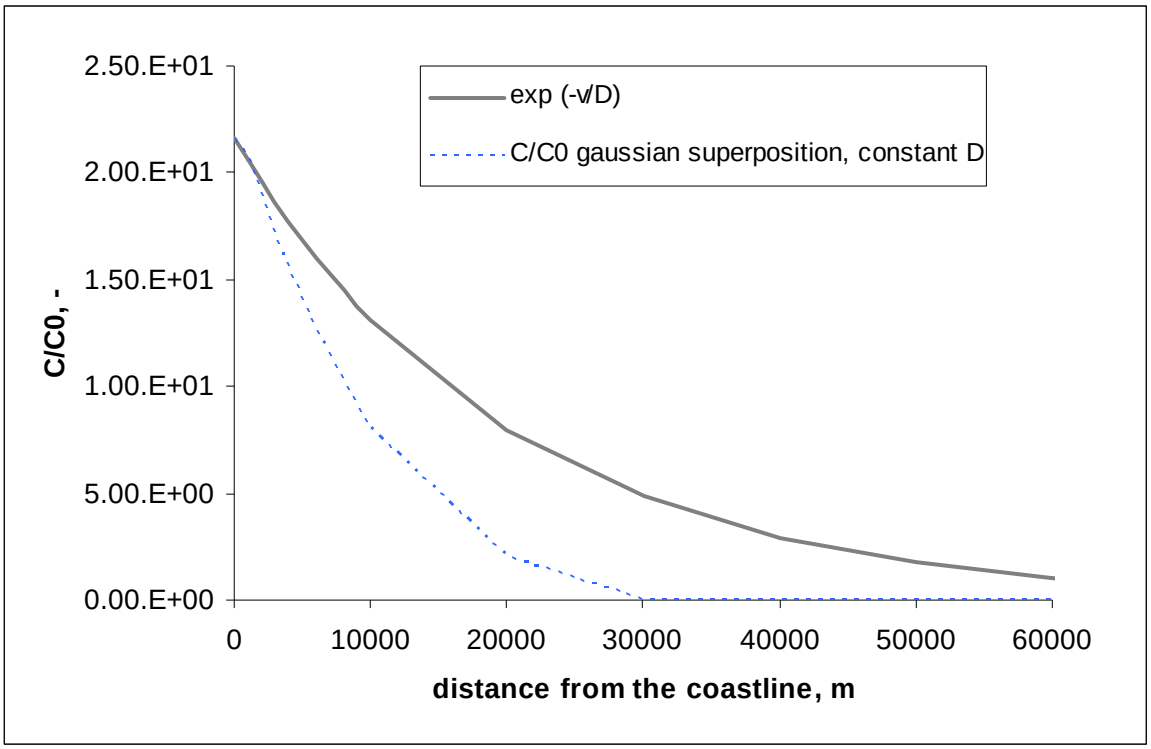

Figure 13 - Spacing 25 m, 200 emissions upstream (5 km)

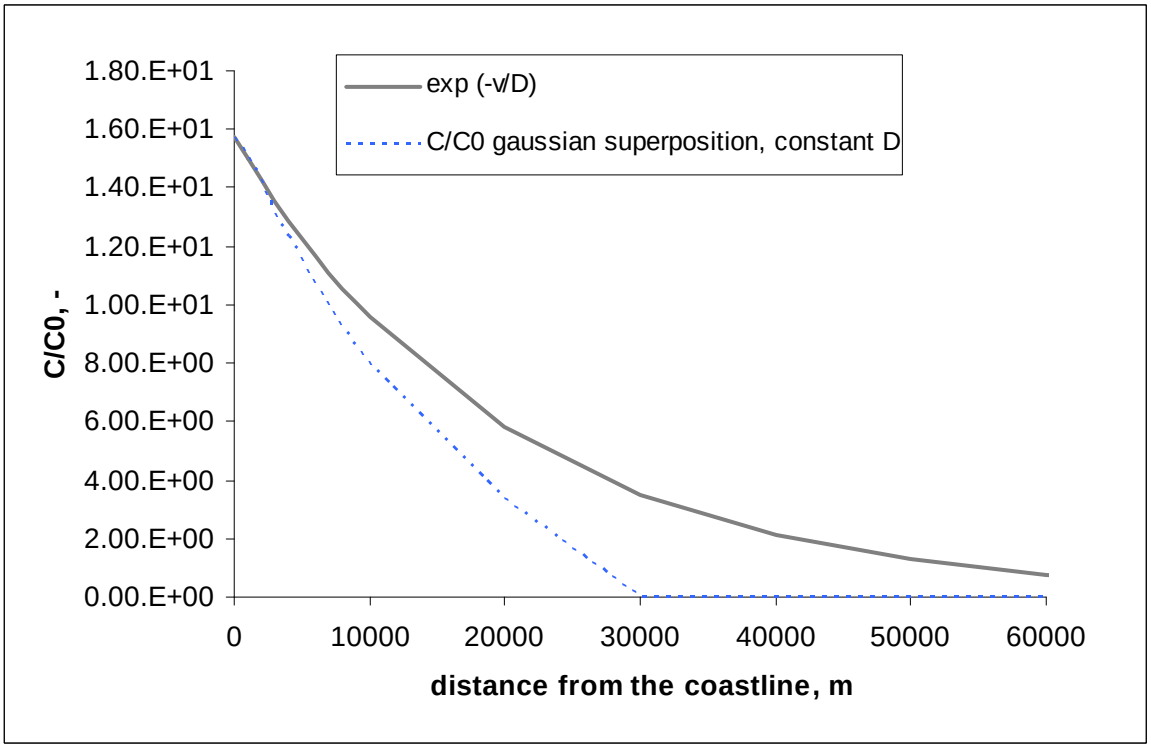

Figure 14 - Spacing 50 m, 200 emissions upstream (10 km)

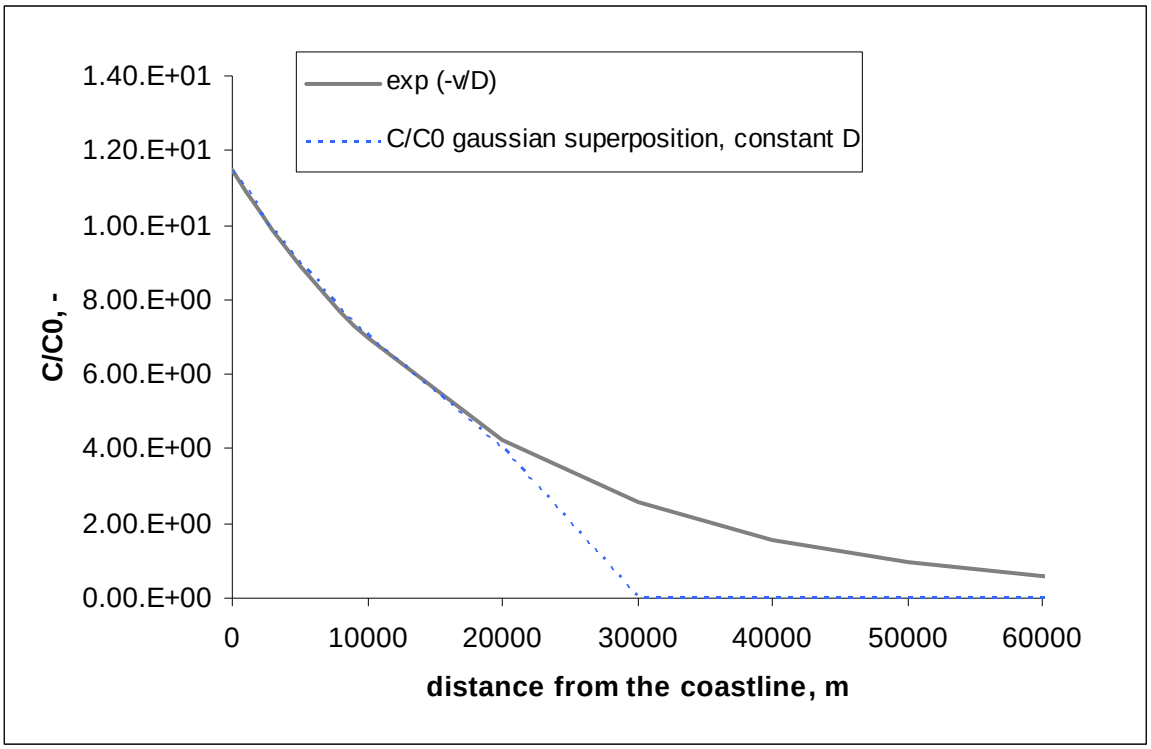

Figure 15 - Spacing 100 m, 200 emissions upstream (20 km)

It is worth stressing that this exponential profile is derived under assumptions completely different from the radial or parallel flow, which yielded equation (10). In light of this property, we can argue that the simple exponential decay with rate v/D is not just an intermediate practical solution for one single emission, between radial and parallel flow, but also a proxy to the solution of the advection-dispersion equation when more emissions are aligned along a straight coastline, with advection parallel to the coastline and dispersion regarded as constant. This provides an additional conceptual scheme that can be used for practical mapping of coastal pollution, when one is interested in a first screening of the observed levels.

Irrespective of its physical interpretation, a simple exponential model seems to capture reasonably the spatial trends of advection and dispersion as a function of distance from the coast. For instance, considering the total suspended matter (TSM) dataset used to parameterize the model, and we plot TSM as a function of the Euclidean distance from the coast (with reference to TSM along the transects shown in Figure 16,which correspond to significant gradients of TSM at river mouths or similar situations), we find an exponential decay as shown in Figure 17. The trend is reasonably approximated by an exponential decay function with rate 4×10^{-5} m^{-1}, as shown in the graph. This value is well in line with the ratio of velocity on dispersion coefficient estimated as explained above.

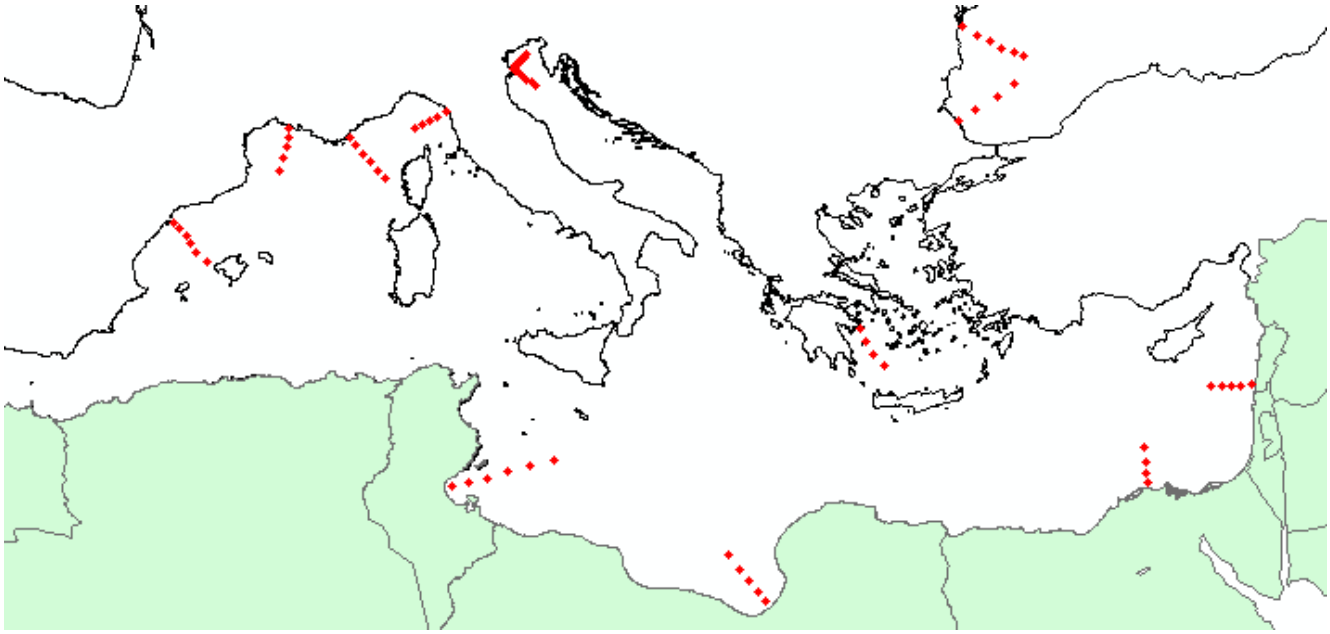

Figure 16 – Profiles for the evaluation of TSM

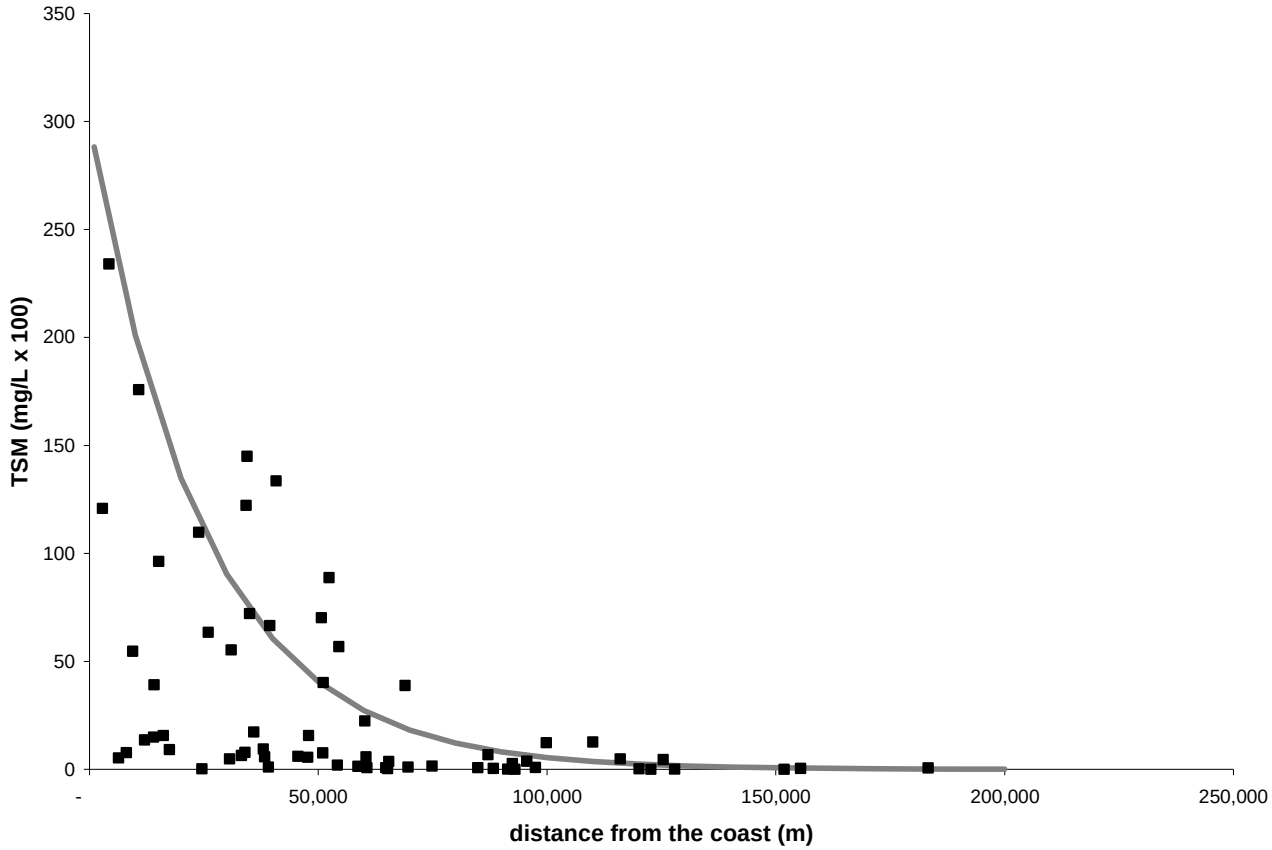

Figure 17 –TSM as a function of distance. The solid gray line represents the exponential decay trend.

In order to test the performance of the exponential decay function of the distance from the coast for screening-level prediction of concentrations, we collected from the literature a few datasets containing measurements of chemical concentration at different distances from the coast, for PFOS and PFOA (data compilation from the North, Mediterranean and Baltic seas provided by courtesy of R. Loos, personal communication), drugs and caffeine measured in the North Sea [57], PAH [8] and TBT [31] measured in the Mediterranean, and Lindane in the North Sea [data reported by 53]. We georeferenced

the sampling locations and we extracted, for each point, the value of the indicator I(x,y) shown in the upper part of Figure 9, and the Euclidean distance from the coast., supposedly occurring near the coast. Then we plotted it together with the measured concentrations normalized by the maximum, as a function of the Euclidean distance from the coast. Results are shown in the following figures. An overall comparison is provided in Figure 22, which indicates clearly that, for screening level calculations, an exponential model based on the indicator I(x,y) generally yields errors within a factor 5. However, there are circumstances where observed concentrations may be higher than predicted by the indicator I(x,y), indicating persistence of high concentrations away from the coast, which can be only explained through a more complex model. This gives an idea of the limits of applicability of the indicator for the screening of coastal pollution.

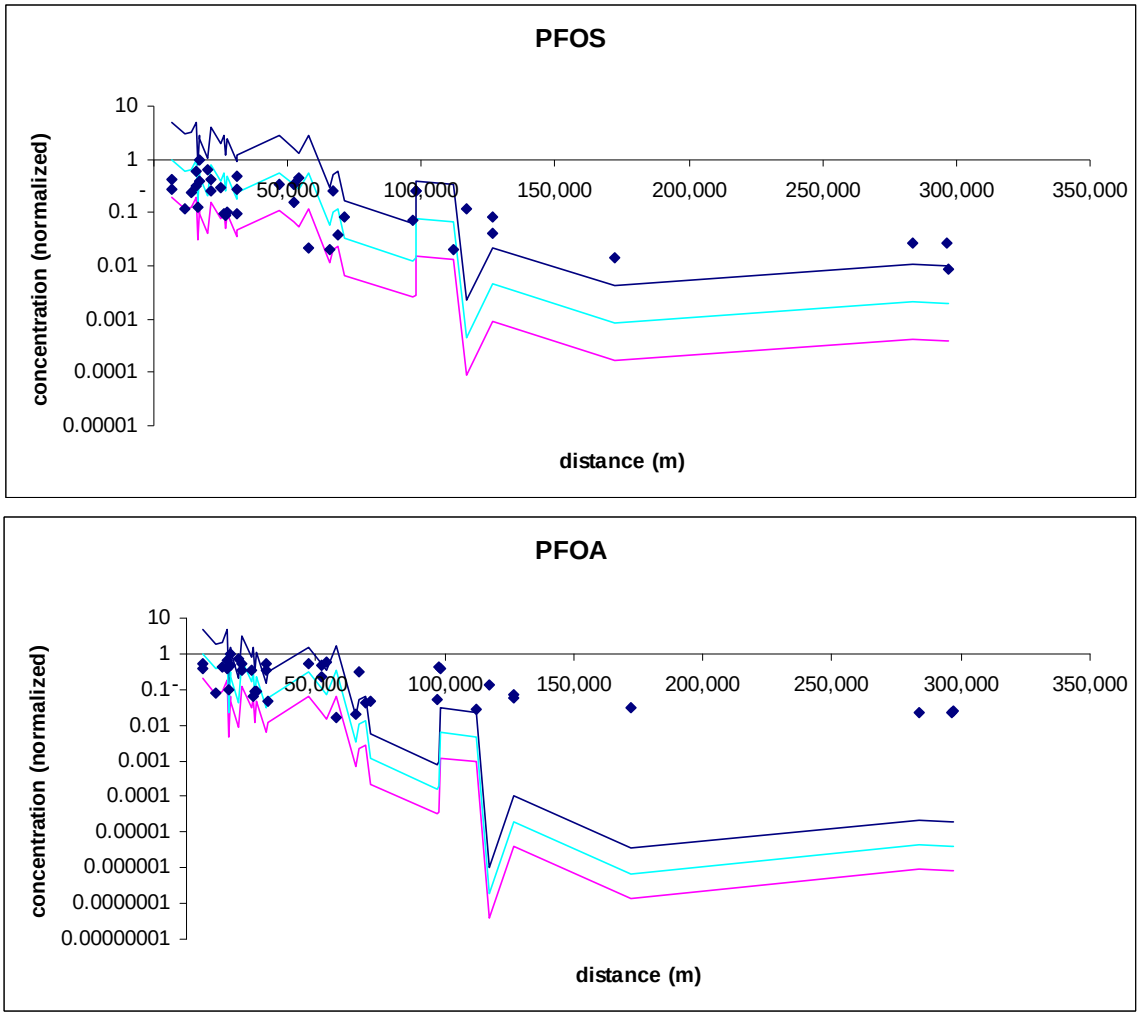

Figure 18 – PFOS and PFOA vs distance from the coast (data compiled by R. Loos, personal communication). Dots represent measurements normalized by the maximum, while lines represent the I(x,y) indicator concentrations, and the same multiplied/divided by a factor 5

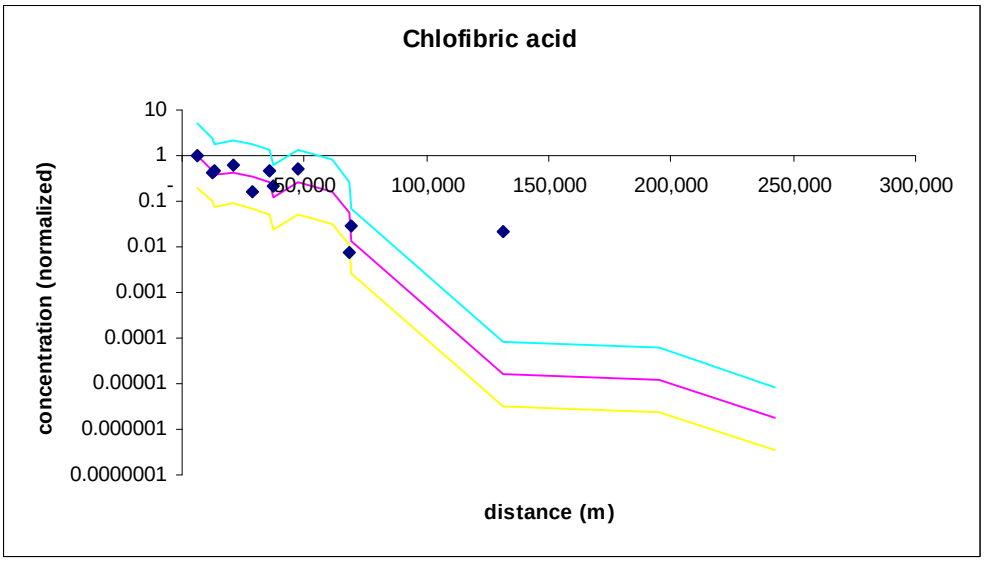

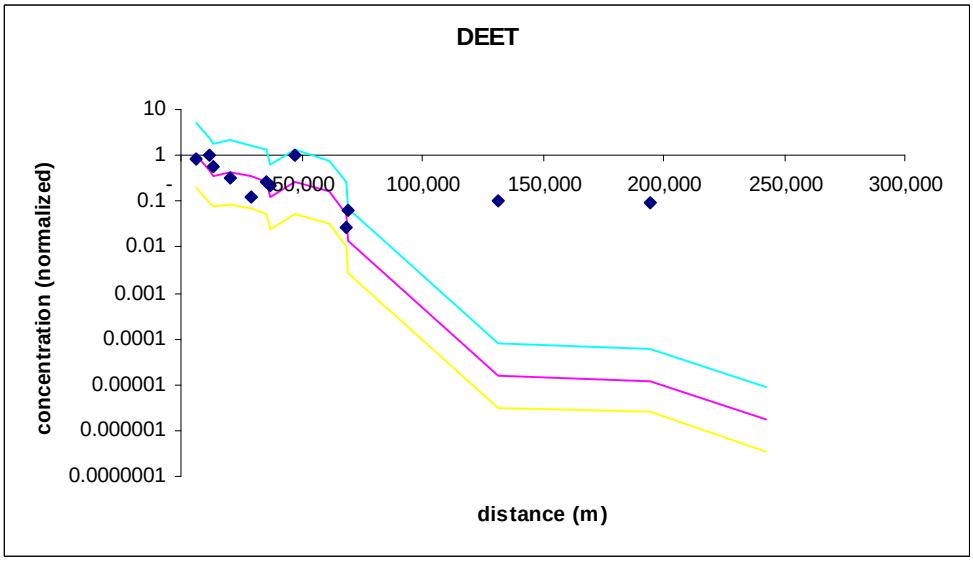

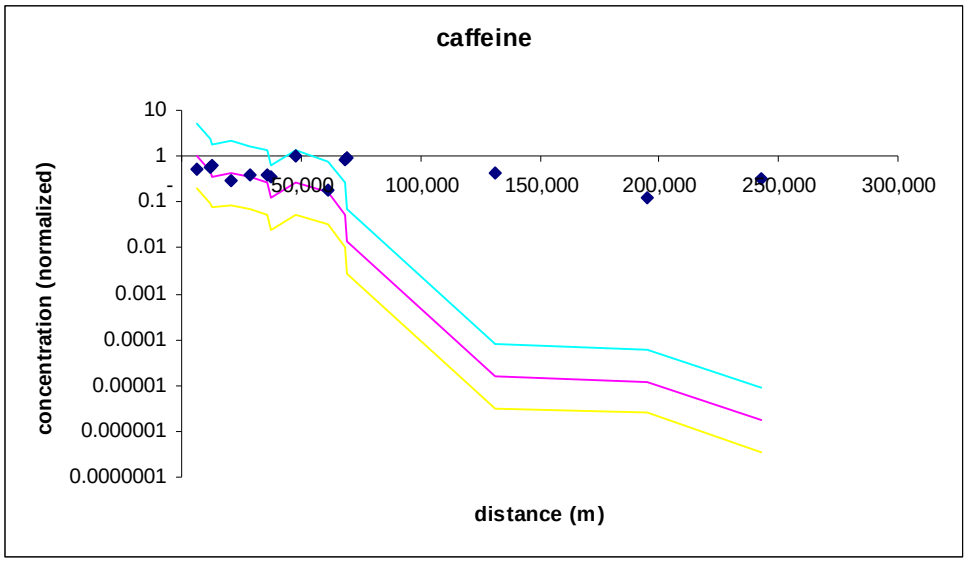

Figure 19 – Concentrations of Chlofibric acid, DEET and caffeine vs distance from the coast [57], North Sea. Dots represent measurements (normalized with respect to the maximum), while lines represent the I(x,y) indicator, and the same multiplied/divided by a factor 5

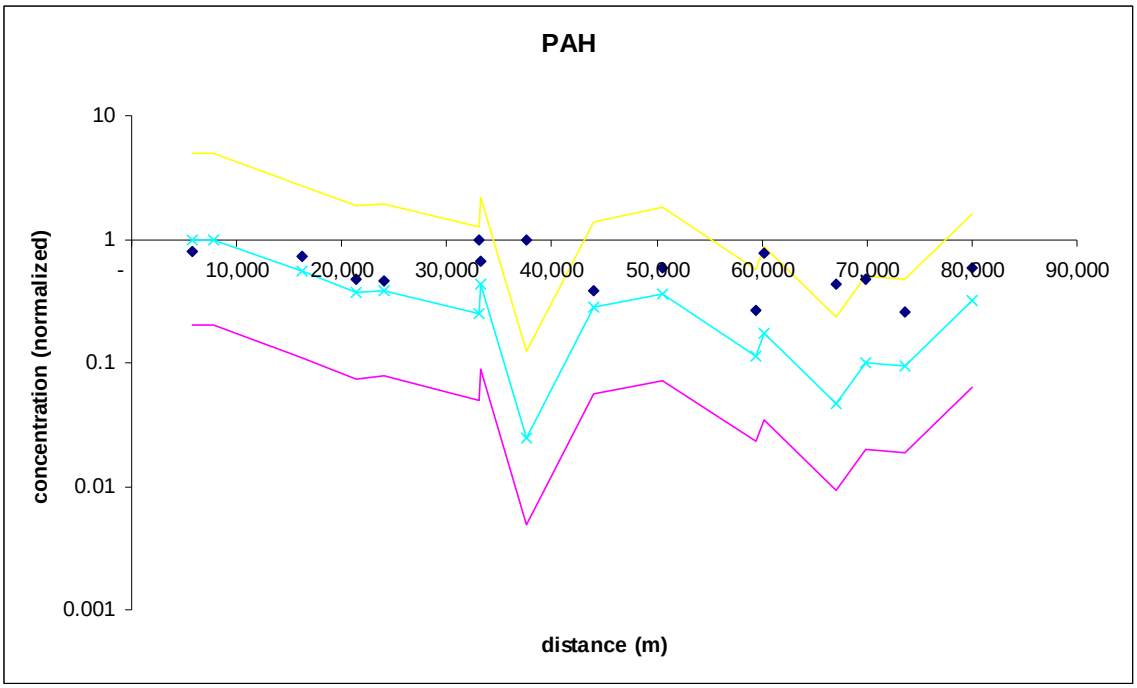

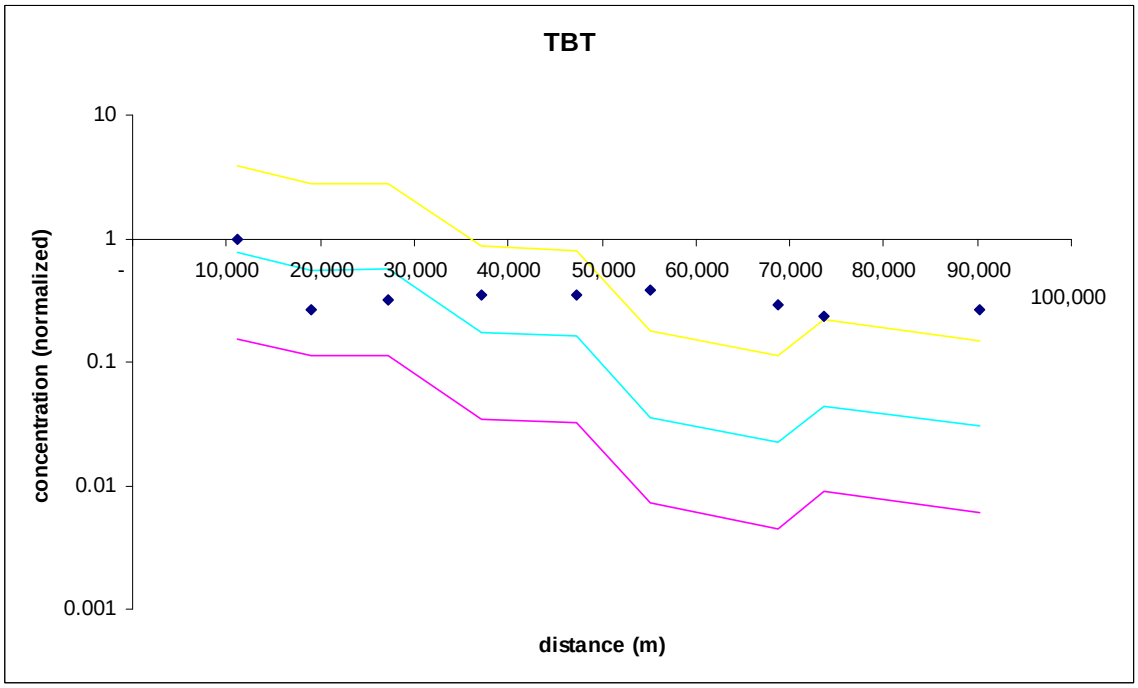

Figure 20 – PAH [8] and TBT [31] vs distance from the coast, Mediterranean. Dots represent measurements (normalized with respect to the maximum), while lines represent the I(x,y) indicator, and the same multiplied/divided by a factor 5

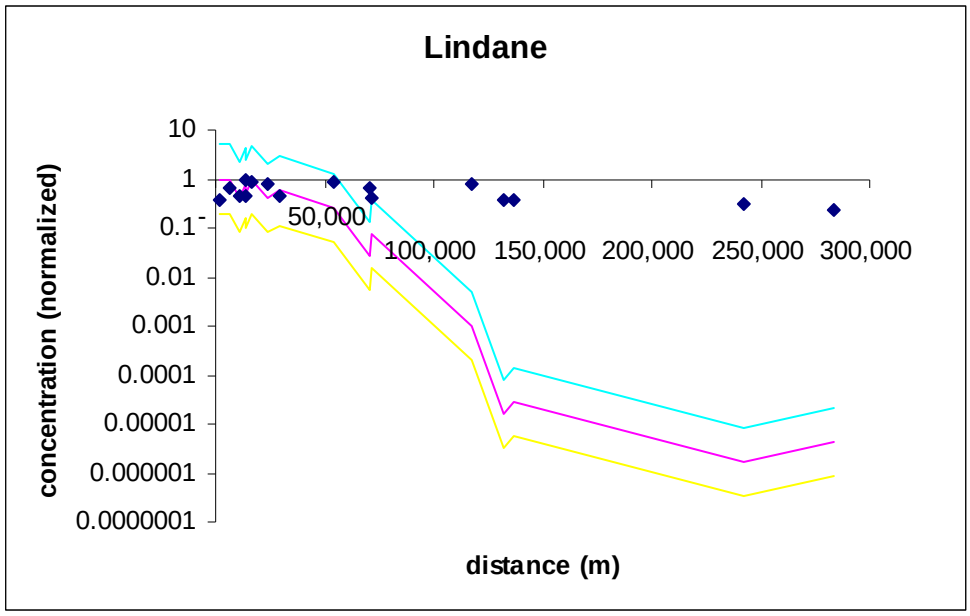

Figure 21 – Lindane [53] vs distance from the coast, North Sea. Dots represent measurements (normalized with respect to the maximum), while lines represent the I(x,y) indicator, and the same multiplied/divided by a factor 5

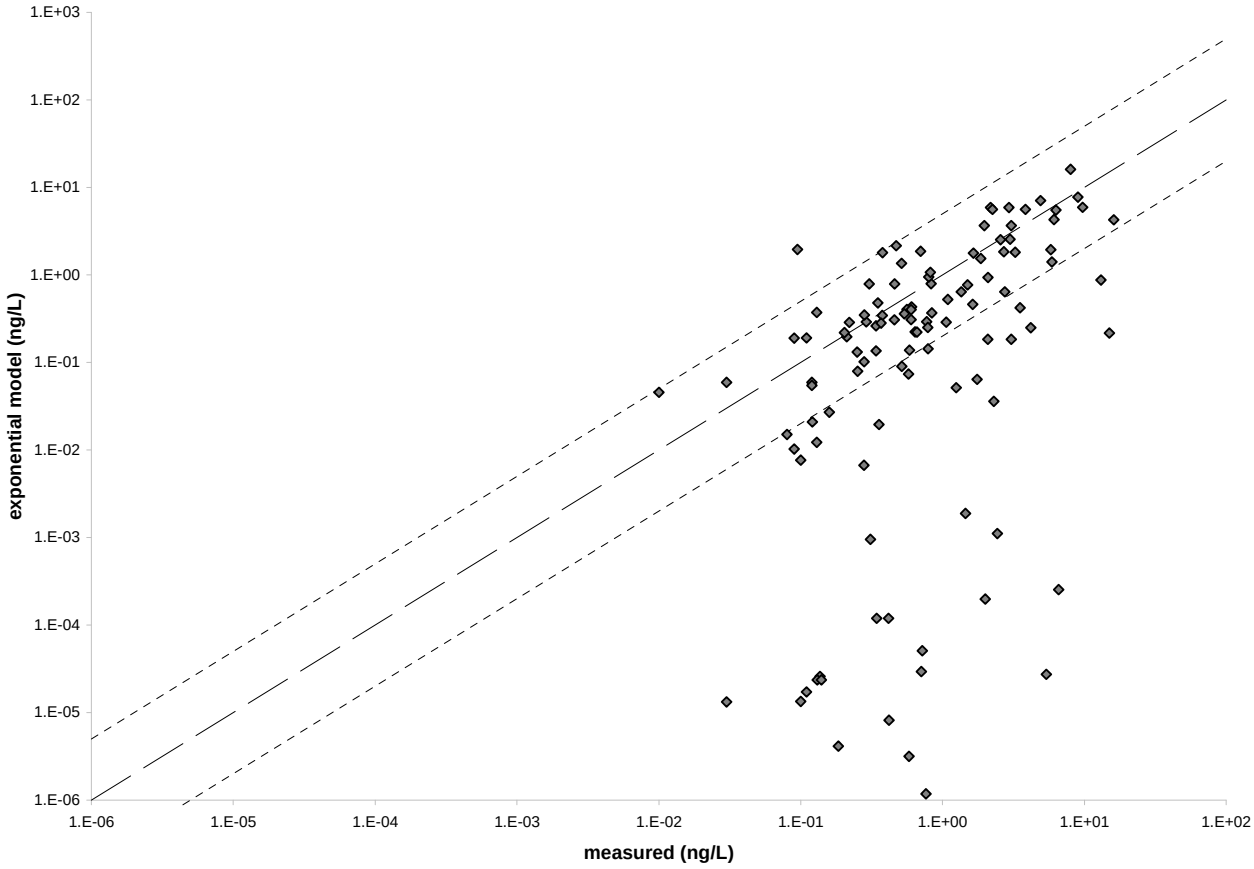

Figure 22 – Comparison of measurements and the exponential model given by I(x,y) multiplied by the maximum concentration in each case.

European Commission

EUR 24267 EN – Joint Research Centre – Institute for Environment and Sustainability
Title: Some considerations on continental scale pollutant transport modelling in European marine waters
Author(s): Pistocchi, A., Stips, A.
Luxembourg: Publications Office of the European Union
2010 – nnnn 38. – 29,7 x 21,0 cm
EUR – Scientific and Technical Research series – ISSN 1018-5593
ISBN 978-9279-15067-8
DOI 10.2788/66854

Abstract

We use the numerical model GETM to build a simplified scheme of pollutant transport for European seas, in form of a linear multiple-box model. Boxes are defined following gyres and still water areas, thus minimizing the number of areas necessary to describe lateral exchanges of contaminants between zones. We use the multiple-box model to identify areas where a “water column” approach can, or cannot, be used for preliminary calculations, depending on the influence of lateral exchanges and the uniformity of distribution of emissions in space. Also, we make use of dispersion and velocity maps to compute the attenuation of coastal pollution for a generic non-conservative pollutant. We show that a reasonable way to compute concentrations as a function of distance from the coast is an exponential decay with constant given by the ratio of velocity on dispersion. The approach is proposed in order to obtain quick estimates of spatial mass distribution of pollutants when a “water column” approach cannot be used, prior to using more comprehensive and computationally demanding sea transport models which remain the elective or necessary tool for more detailed evaluation.

How to obtain EU publications

Our priced publications are available from EU Bookshop (http://bookshop.europa.eu), where you can place an order with the sales agent of your choice.

The Publications Office has a worldwide network of sales agents. You can obtain their contact details by sending a fax to (352) 29 29-42758.

LB-NA-24267-EN-C

The mission of the JRC is to provide customer-driven scientific and technical support for the conception, development, implementation and monitoring of EU policies. As a service of the European Commission, the JRC functions as a reference centre of science and technology for the Union. Close to the policy-making process, it serves the common interest of the Member States, while being independent of special interests, whether private or national.

Publications Office
Publications.europa.eu

ISBN 978-92-79-15067-8